

Development of a sapphire microstrip detector for gamma beam monitoring

16th Pisa Meeting on Advanced Detectors
28 May 2024 – Isola d'Elba (Italy)

Speaker: *Pietro Grutta* (grutta@infn.it) on behalf of the GBP group:

G.Avonj^[1], M.Benettoni^[2], M.Bruschi^[1], N.Cavanagh^[3], F.Dal Corso^[2], U.Dosselli^[2], K.Fleck^[3], E.Gerstmayr^[3], M.Giorato^[2], P.Grutta^[2], F.Lasagni Manghi^[1], S.Mattiazzo^[2], M.Morandin^[2], D.Pantano^[2], G.Sarri^[3], A.Sbrizzi^[1], S.Vasiukov^[2], M.Zuffa^[1]

^[1]INFN and University of Bologna, Bologna (Italy)

^[2]INFN and University of Padova, Padova (Italy)

^[3]School of Mathematics and Physics, The Queen's University of Belfast, Belfast (UK)

LUXE



HELMHOLTZ





Table of contents

Introduction

- LUXE in a nutshell
- LUXE experimental setup and the GBP
- GBP. Rationale and requirements

Sapphire R&D

- Overview of the R&D campaign
- Quality inspection of sapphire sensors
- Detector characterization. CCE. Theory
- Sensor response investigation: from prototypes (pad, 4 strips) to the 192-strip sensor.

Selection of the main results for

- CCE(V)

CCE(Q)

- Detector resolution
- Radiation damage

LUXE TDR

<https://arxiv.org/abs/2308.00515>

LUXE in a nutshell

■ LUXE is an experiment at DESY to perform precision measurements of the transition into the non-linear regime of strong field quantum electrodynamics (SFQED), and to search for new particles beyond the Standard Model coupling to photons.

■ **SFQED physics** relevant for:

■ Astrophysics

- ▶ highly magnetized stars
- ▶ propagation of cosmic rays

■ Nuclear physics

- ▶ of heavy nuclei ($Z > 137$)

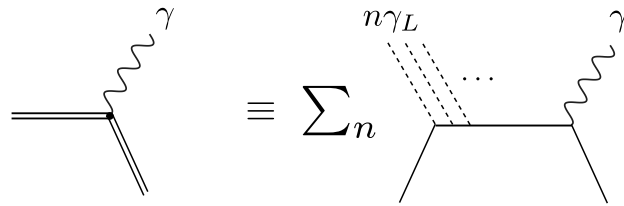
■ Particle physics of future colliders

- ▶ Beam-beam lepton collisions

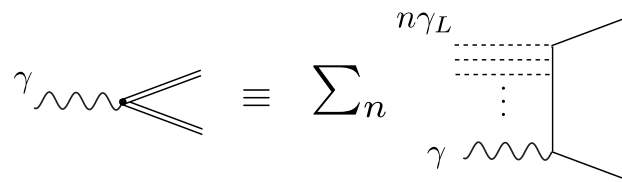


LUXE in a nutshell

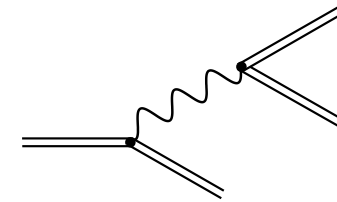
- LUXE is an experiment at DESY to perform precision measurements of the transition into the non-linear regime of strong field quantum electrodynamics (SFQED), and to search for new particles beyond the Standard Model coupling to photons. The onset of **SFEQ** is probed
 - with the **processes** NLC, NBW and NTP,



$e^{\pm} + n \gamma_L \rightarrow e^{\pm} + \gamma$
 Nonlinear inverse Compton
NLC



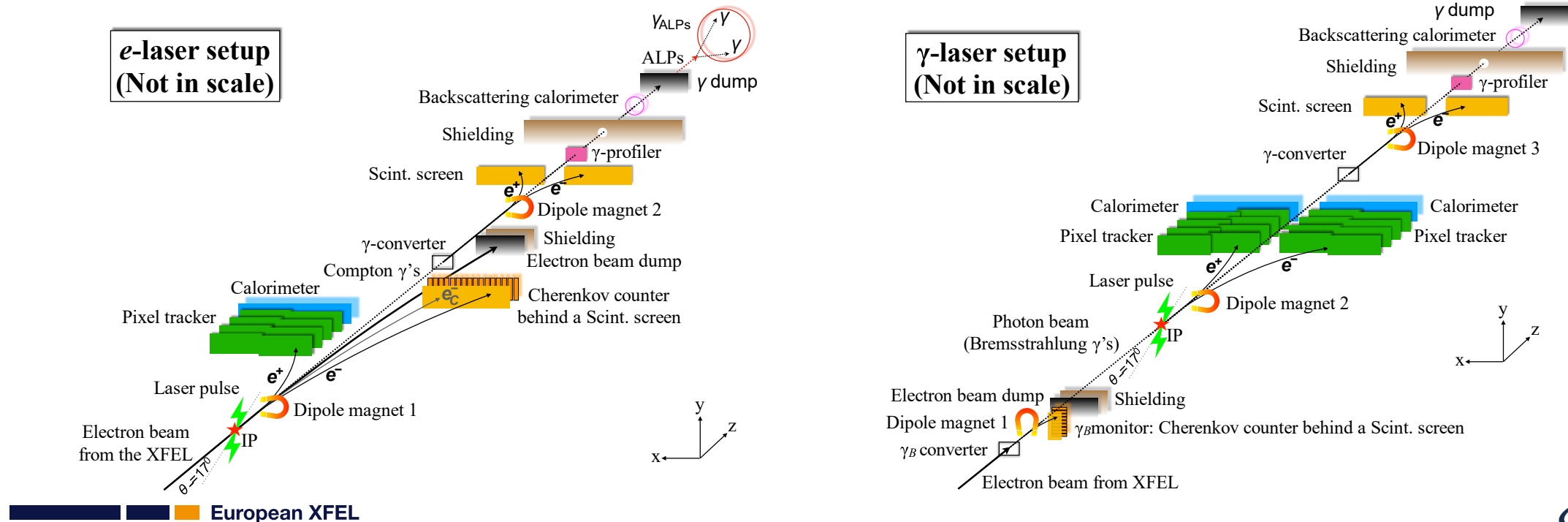
$\gamma + n \gamma_L \rightarrow e^+ + e^-$
 Nonlinear Breit-Wheeler
NBW



$e^{\pm} + n \gamma_L \rightarrow e^{\pm} + \gamma$
 $\gamma + n' \gamma_L \rightarrow e^+ + e^-$
 Nonlinear Trident
NTP

LUXE experimental setup

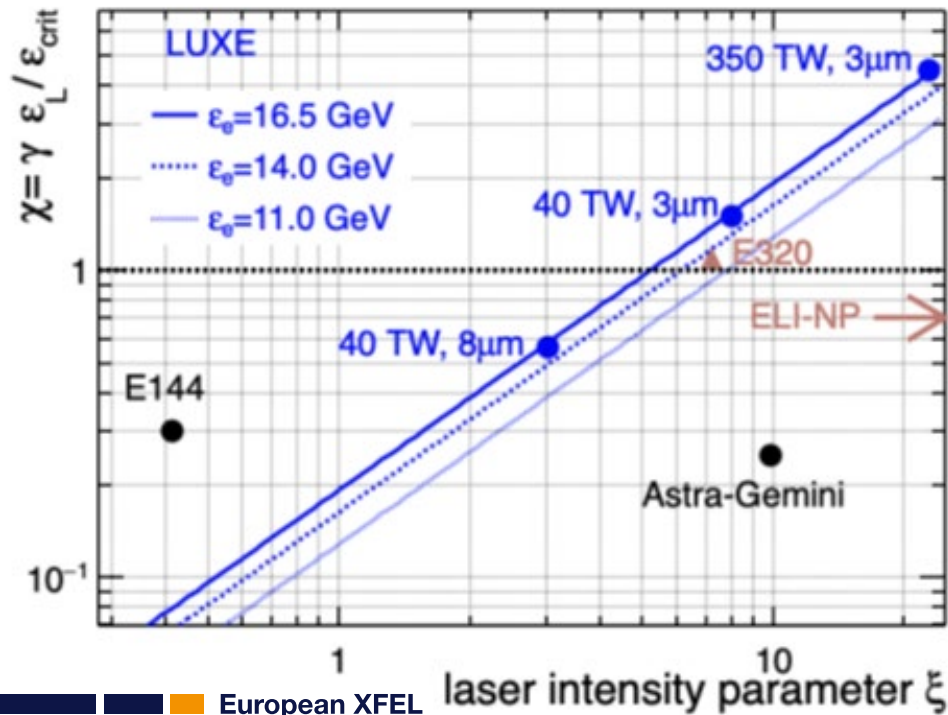
- LUXE is an experiment at DESY to perform precision measurements of the transition into the non-linear regime of strong field quantum electrodynamics (SFQED), and to search for new particles beyond the Standard Model coupling to photons. The onset of **SFEQ** is probed
 - with the **processes** NLC, NBW and NTP,
 - by **colliding** 16.5GeV e^- with a 40-350TW laser beam:



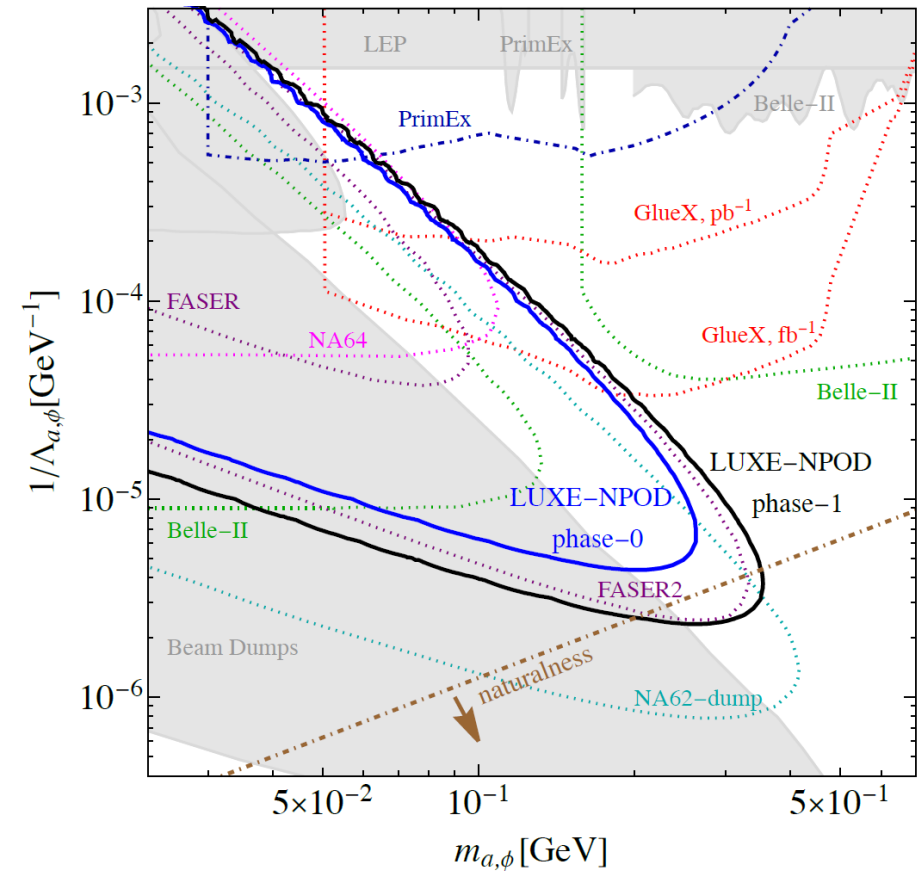


LUXE key features

- Collaboration of *particle* and *laser* physics communities.
- First obs. of e^+, e^- pair prod. *tunnelling out of the vacuum* in EM field above the Schwinger limit.

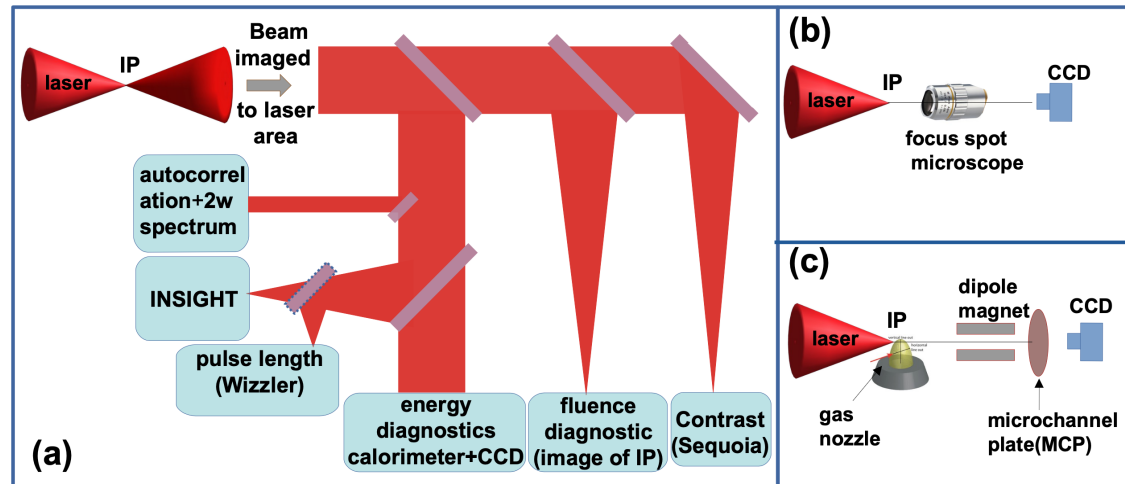


- High intensity high energy gamma beam (used for ALP searches coupling with γ)

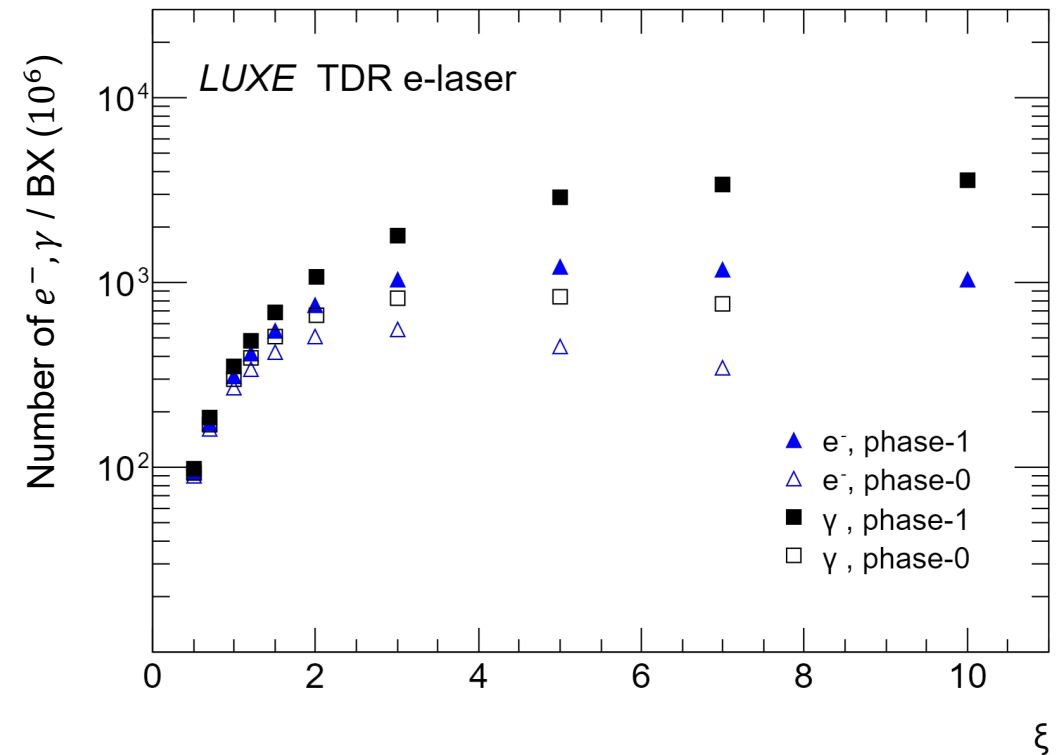


LUXE challenges

- Precise time/spatial *overlap* of e-laser beams, high laser *stability* and novel *diagnostic* (laser).

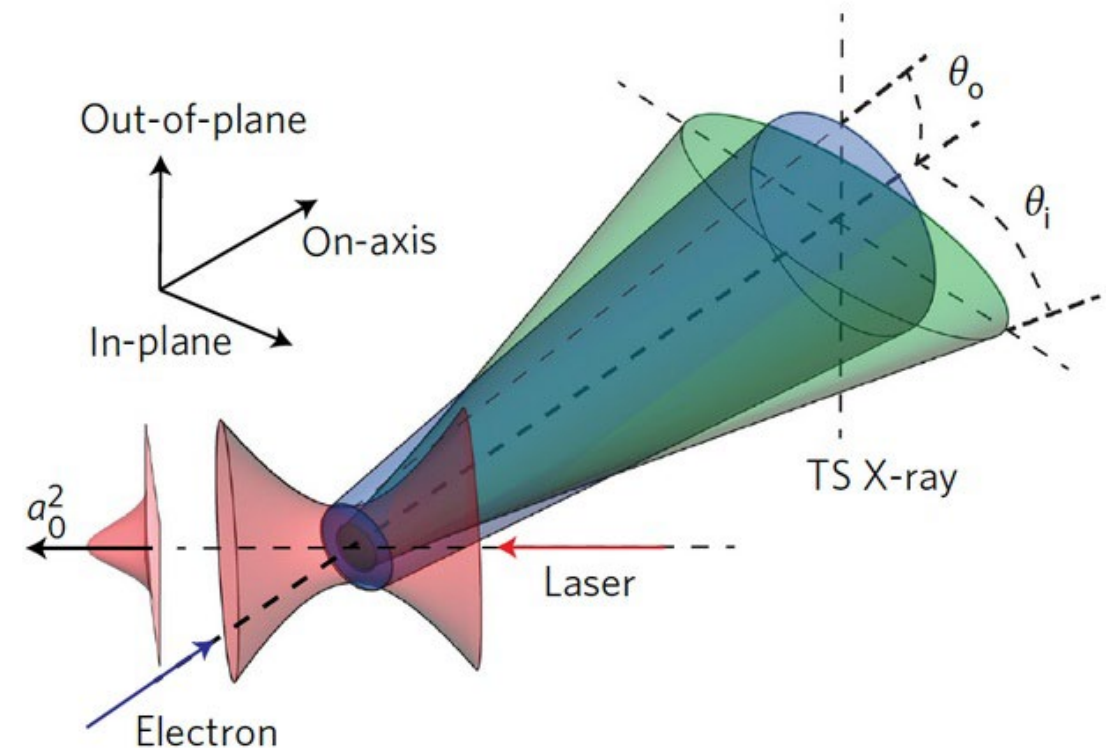


- Wide range of particle production rates (from $10^{-2} e^+$ to $10^9 \gamma$ per event): *high energy fluences* and *high dynamic range* signals.



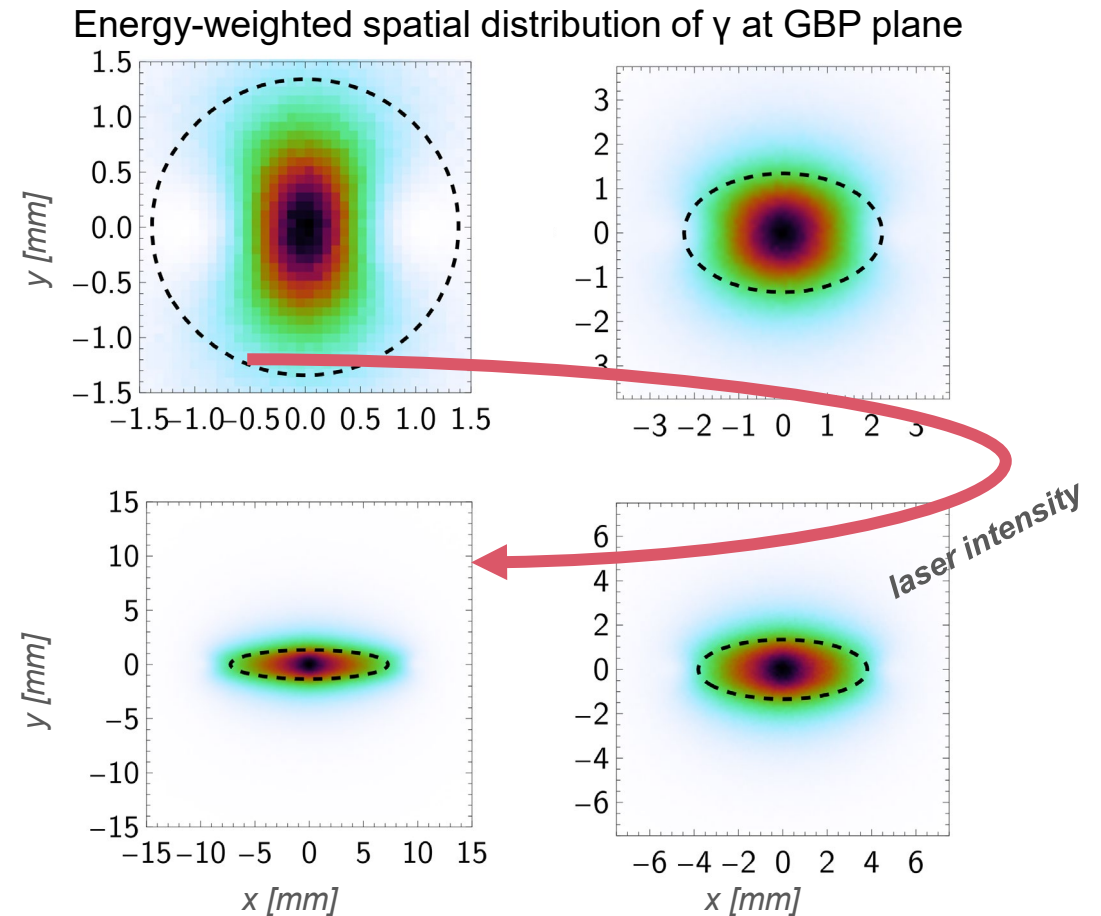
Gamma Profiler in LUXE. Rationale

- NLC angular/spectral distributions are **strongly dependent on the laser intensity ξ** , whose measure is fundamental.
- Laser diagnostic and other typical approaches are limited in shot-to-shot measurement.



Gamma Profiler in LUXE. Rationale

- NLC angular/spectral distributions are **strongly dependent on the laser intensity ξ** , whose measure is fundamental.
- Laser diagnostic and other typical approaches are limited in shot-to-shot measurement.
- A model independent **online** measure of the laser intensity can be retrieved by the angular distribution of the Compton photons.





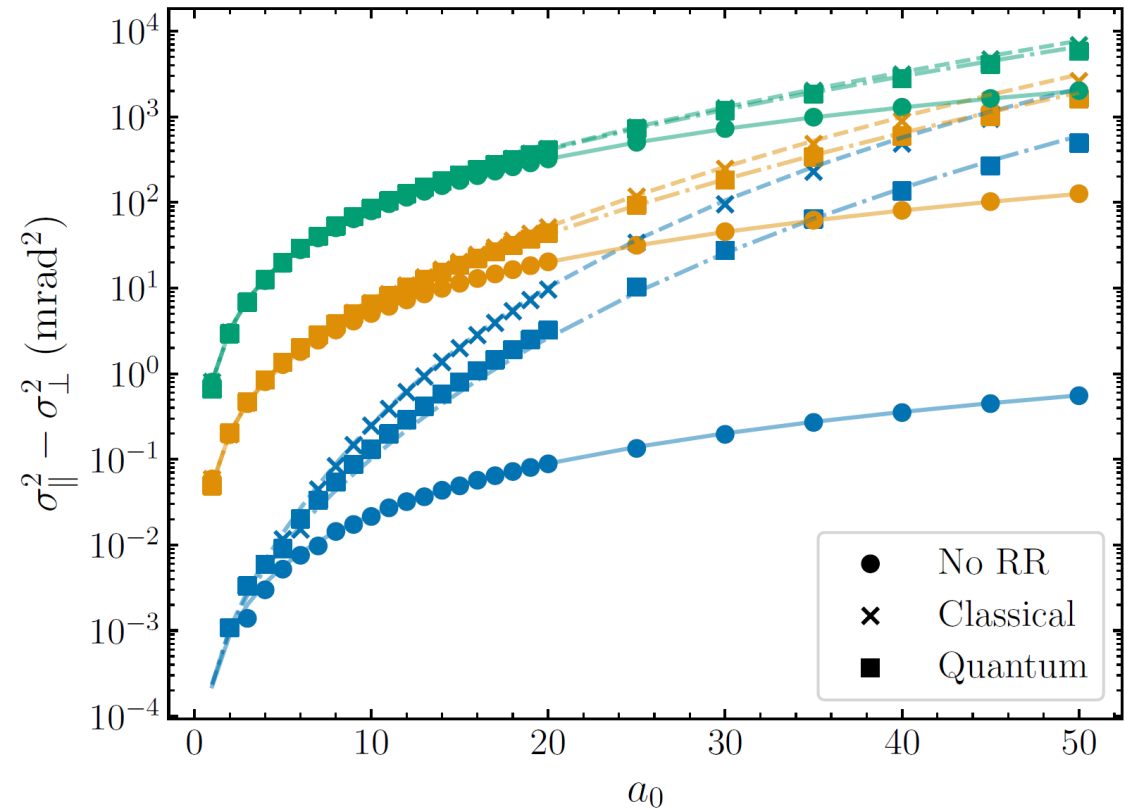
Gamma Profiler in LUXE. Rationale

- NLC angular/spectral distributions are **strongly dependent on the laser intensity ξ** , whose measure is fundamental.
- Laser diagnostic and other typical approaches are limited in shot-to-shot measurement.
- A model independent **online** measure of the laser intensity can be retrieved by the angular distribution of the Compton photons.
- For a linearly polarised laser, in the **difference**

$$\sigma_{\parallel}^2 - \sigma_{\perp}^2 = \frac{a_0^2}{3 \kappa_1} \left[\left\langle \frac{1}{\gamma_i} \right\rangle \left\langle \frac{1}{\gamma_f} \right\rangle + \kappa_2 \left(\left\langle \frac{1}{\gamma_f^2} \right\rangle + \left\langle \frac{1}{\gamma_i^2} \right\rangle - 2 \left\langle \frac{1}{\gamma_f} \right\rangle \left\langle \frac{1}{\gamma_i} \right\rangle \right) \right]$$

$$\equiv \frac{a_0^2}{3 \kappa_1} f(\gamma_i, \gamma_f; \kappa_2)$$

of the **beam profile width** along the parallel and perp. directions w.r.t. the laser polarisation axis. (κ const.s)



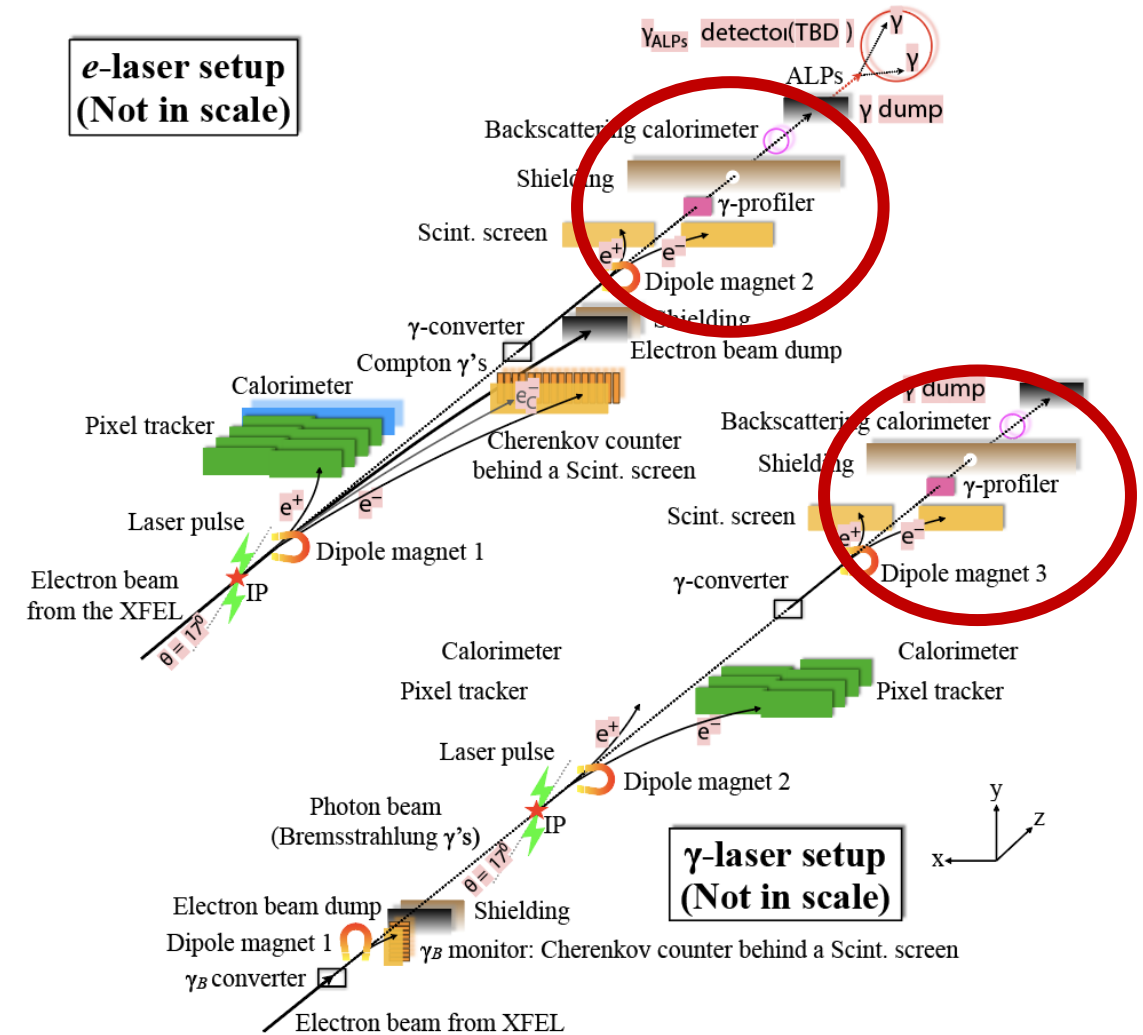
Difference in the parallel/perp. variance w.r.t. the laser pol. axis of the emitted radiation profile by an electron beam with central energy E and 1% RMS energy spread, and divergence 1 mrad for E=250 MeV (green); E=1 GeV (orange); and E=15 GeV (blue) as predicted by $f(\gamma_i, \gamma_f; \kappa_2)$ (lines) and calculated from LCFA simulations (points).

from <https://arxiv.org/abs/2402.03454>

Introduction. GBP in LUXE detectors

- The GBP detector is part of the LUXE's gamma detection system (gamma spectrometer, profiler and flux monitor) in both e-laser and γ -laser setups.
- The GBP is placed along the beamline at around **11.5m downstream the IP**, with the purpose of measuring the spatial distribution of the photons and tagging the (e⁻ beam)-laser misalignment.

- **Gamma Beam Profiler** has the purpose of measuring the Compton beam with desired **O(10 μ m) precision** for ξ reconstruction within 2.5%.



Introduction. Requirements

- Scientific goal of laser intensity retrieval with a relative uncertainty up to 2.5%

$$\frac{\delta\xi}{\xi} \simeq \sqrt{\frac{1}{4} \left(\frac{\delta k}{k}\right)^2 + \frac{\sigma_{\parallel}^2 + \sigma_{\perp}^2}{(\sigma_{\parallel}^2 - \sigma_{\perp}^2)^2} (\delta\sigma)^2} \quad \text{with} \quad \frac{\delta k}{k} \simeq 1\%$$

implies beam profile reconstruction with **<10 μm** spatial resolution for the GBP for $\xi > 1$.

- Physics of the process resulting in large variations for $\frac{d^2 N_{\gamma}}{d\theta_{\parallel} d\theta_{\perp}}$ which implies **signals with high dynamic range**.
- High photon energy rate ($\sim 10^9 \text{ GeV s}^{-1}$) require a **radiation-hard material**.

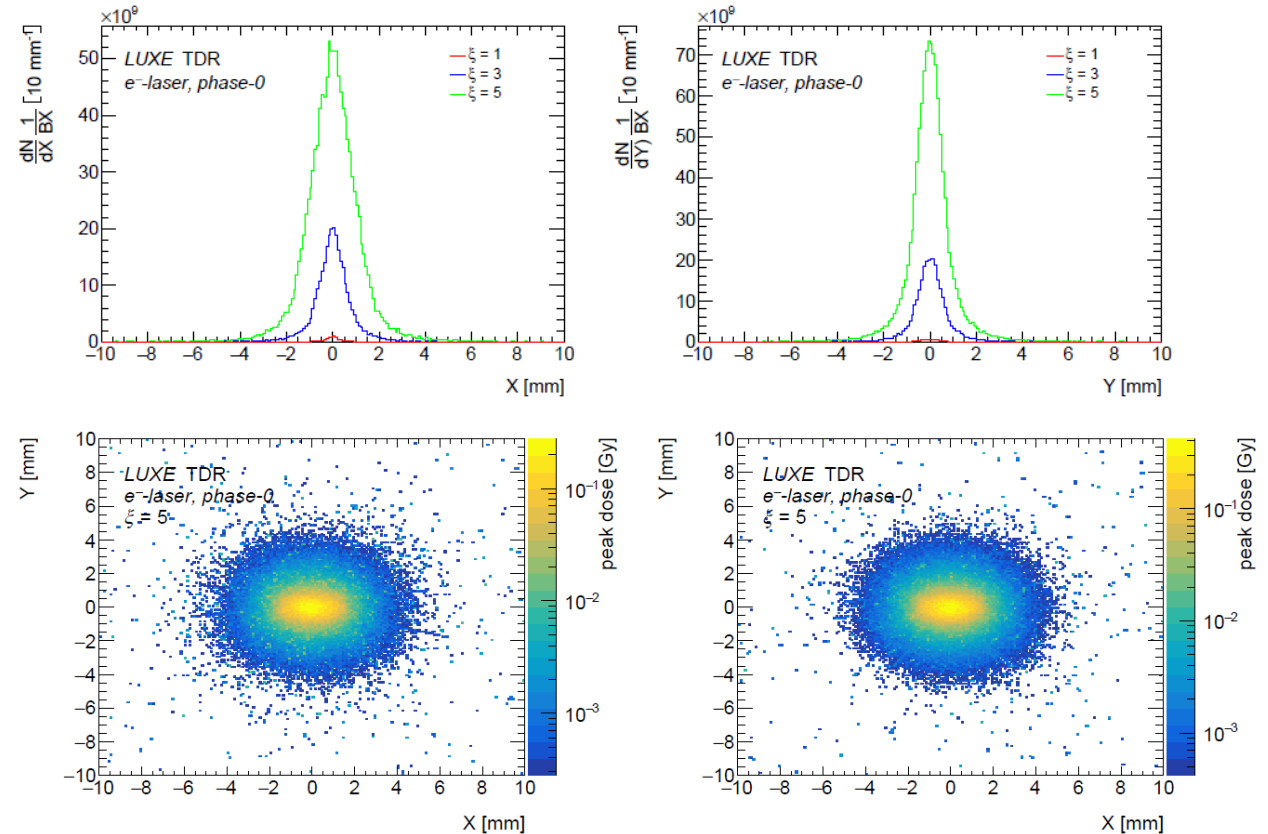


Figure 15: Dose distribution profile for the upstream (left) and downstream (right) detectors. Energy depositions from the Compton beam signal are considered. Points where no depositions occurred are blank.



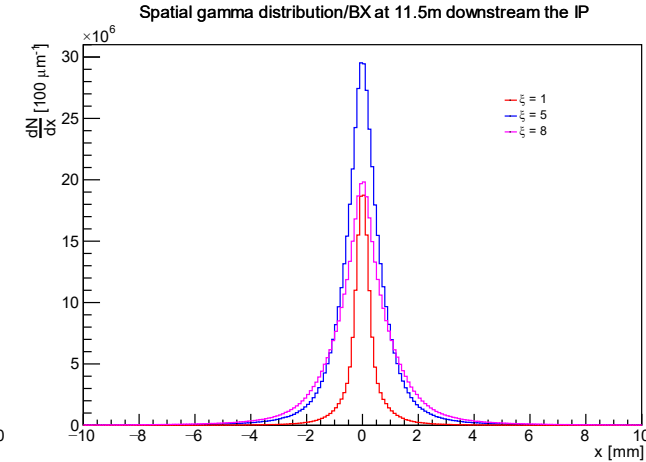
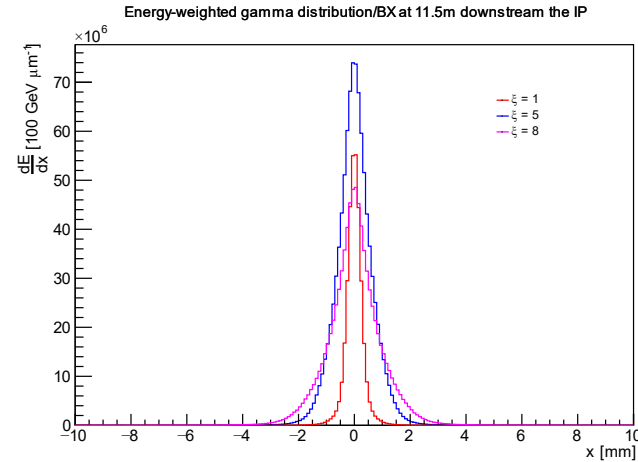
Introduction. Why sapphire? (in a nutshell)

- Artificial sapphire gained some interest as radiation detector in radiation harsh environments for beam condition monitor applications as a cheaper flexible candidate alongside pCVD diamond detectors.

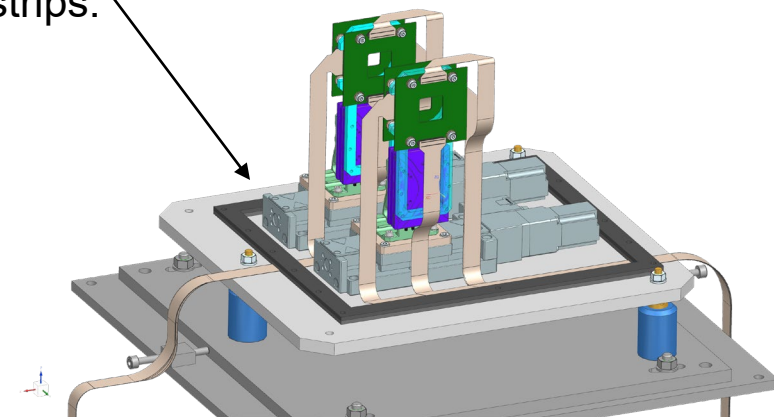
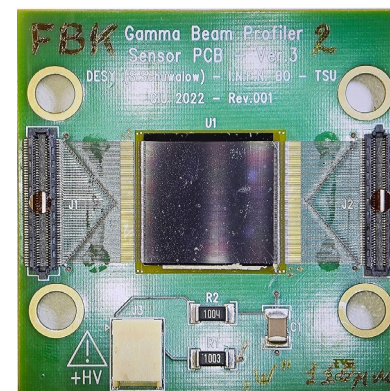
Property	Silicon	Diamond	Sapphire ^{[1] [2]}	
Density [g cm ⁻³]	2.33	3.52	3.99	
Band gap [eV]	1.12	5.5	9.9	Insulator, solar blindness
Displ. Energy [eV]	13-20	43	79	Radiation-hard material
Relative permittivity	11.7	5.7	9.3-11.5	
Breakdown [kV cm ⁻¹]	3 10 ²	10 ⁴	4 10 ²	HV operation
Resistivity [Ω cm]	10 ⁵	10 ¹⁶	10 ¹⁶	Very low (~pA) leakage current
Energy / eh-pair [eV]	3.6	13	27	
Mobility e- (T _{amb}) [cm ² V ⁻¹ s ⁻¹]	1400	2800	600	Chg. collection mainly due to electronic transport
MIP [eh μm ⁻¹]	73	36	22	Relatively small signals w.r.t. diamond
Rad. Length [cm]	9.4	12.2	7.0	

Introduction. Summary of the detector proposal

- Photon's angular profile required for a_0 inference requires measuring $\theta_{\parallel} < 2 \frac{a_0}{\langle \gamma_f \rangle}$.
- For typical LUXE parameters ($a_0 < 7.9$ phase-0, $a_0 < 23.6$ phase-1), at 11.5m downstream the interaction point the beam profile spans the range $|x_{\parallel}| < 7.30\text{mm}$ (ptarmigan LMA + RR $w_0=2.95\mu\text{m}$)
- Requirements on spatial resolution and detector constrains (rad. hardness), combined with the aim to use custom non rad-hard front-end electronics, have led to a detector proposal with a **strip** readout design – i.e. with a **sapphire** sensor covering range **20x20 mm²** with a **pitch of 100 μm** .
- Detector design involves two redundant xy-stations

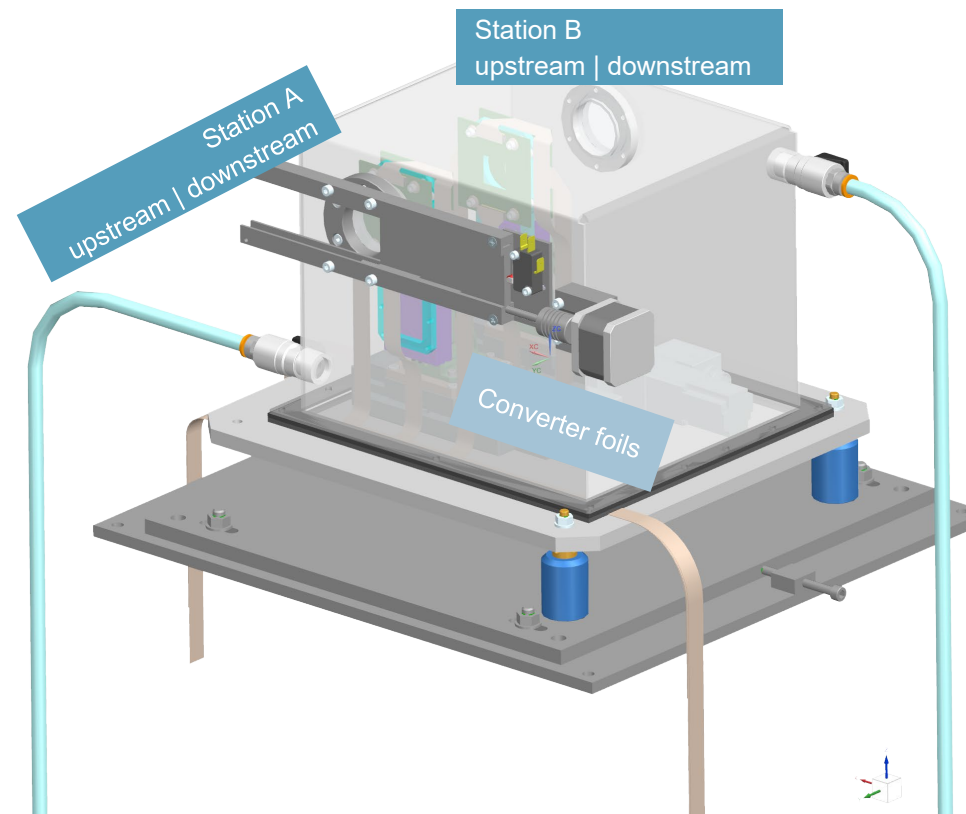
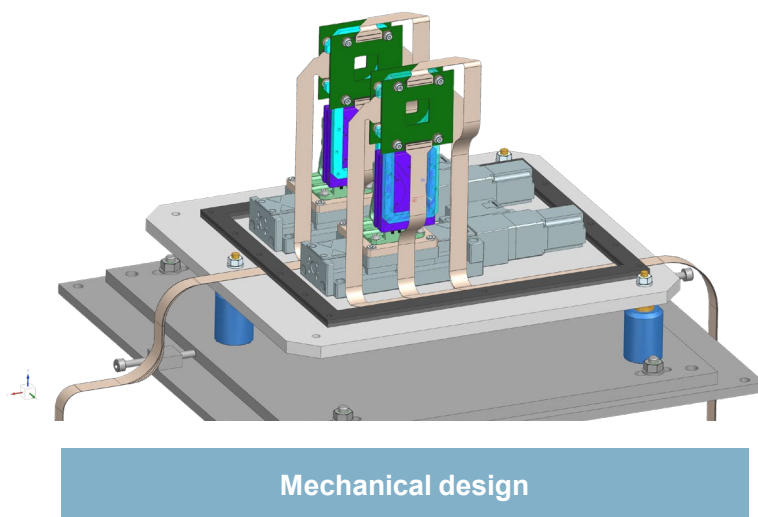


(each instrumented with 2 sapphire sensors) with motorized stages – i.e., to be able to move in/out beam and calibrate the strips.



System overview. Mechanics

- Each station is equipped with 2 orthogonally-placed 192-strip sapphire detectors, mounted on μm -precision movable XY actuators with 25mm travel each.



- Motor stages moved away from the beam XZ plane, to reduce dose delivered.
- Converter materials before the entrance window, to improve signal at low ξ
- Detector enclosed in a Faraday shield, acting also as gas enclosure: dry air / nitrogen may be used to preserve cleanliness.
- Entry/exit polyimide windows, optionally aluminised with thickness as low as $13\mu\text{m}$.



Sapphire R&D

Overview. Quality control and Test beams. Rationale

- An experimental campaign has been carried out to investigate sapphire properties as radiation detector, and to validate the detector design with various prototypes: pad-sensor, 4-strip, 192-strip sensors.
- Sapphire wafers **quality control** and inspection.
- **Objectives:**
 1. Charge collection efficiency as a function of the biasing voltage → **CCE(V) pad-sensor prototype**
 2. CCE(V), strip uniformity & relative eff. as a function of the absorbed dose → **1st rad.-damage study & bare signal measure 4-strip**
 3. **Full system test** (PSU, FERS-A5202) of the final detector design **resolution with 192-strip (early sapphire batches)**
 4. **Final 192-sensors** final batches (strips made in Italy by FBK) **2nd rad.-damage + resolution (WIP)**

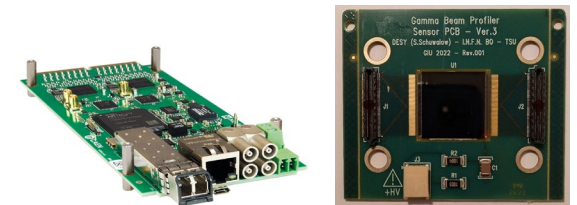
Sapphire pads
(INFN-LNF)



Sapphire 4-strip
(CERN)

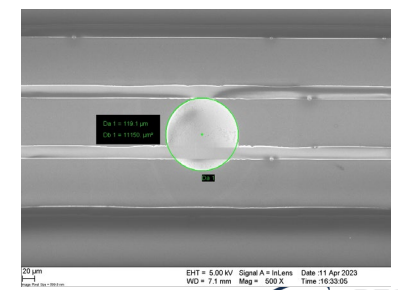
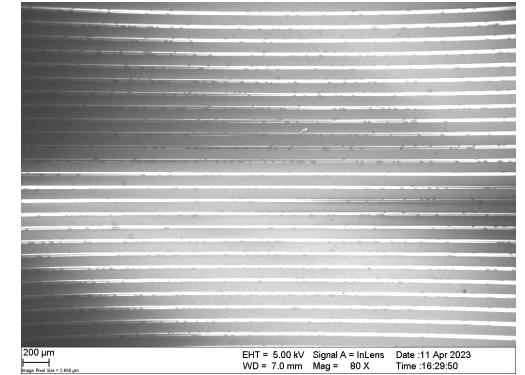
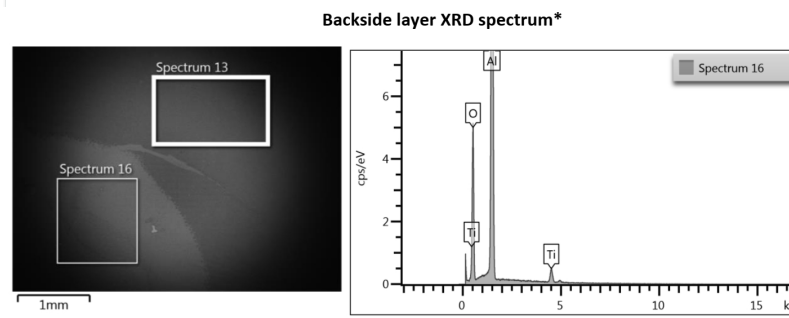
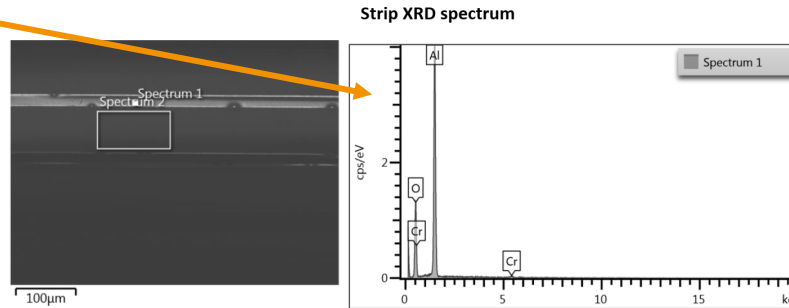
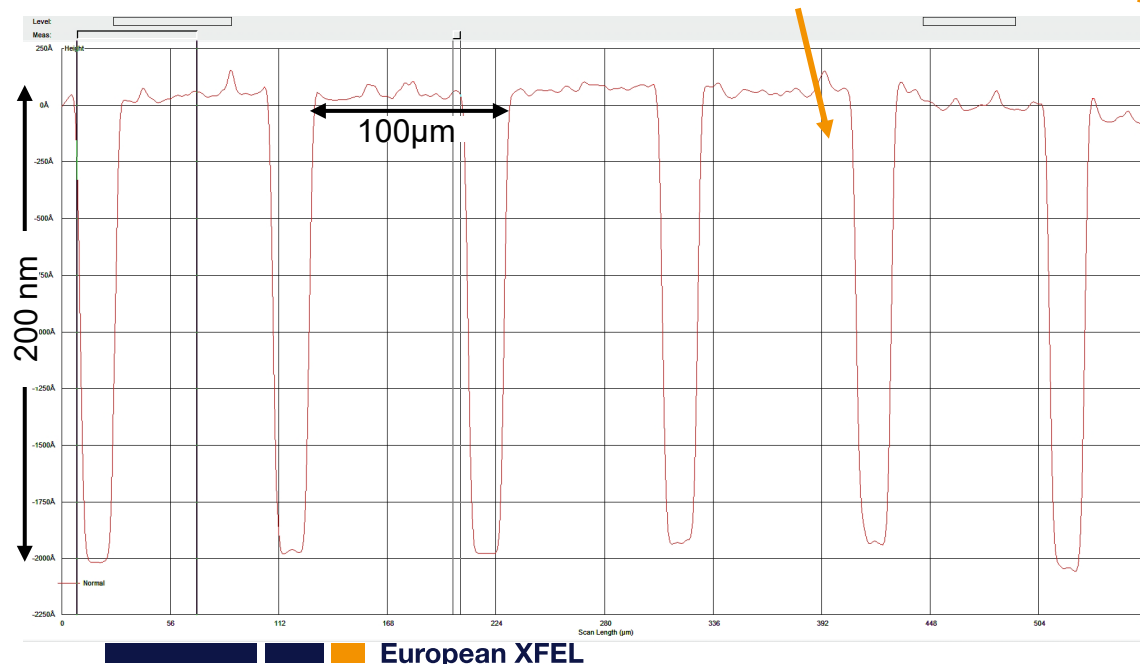
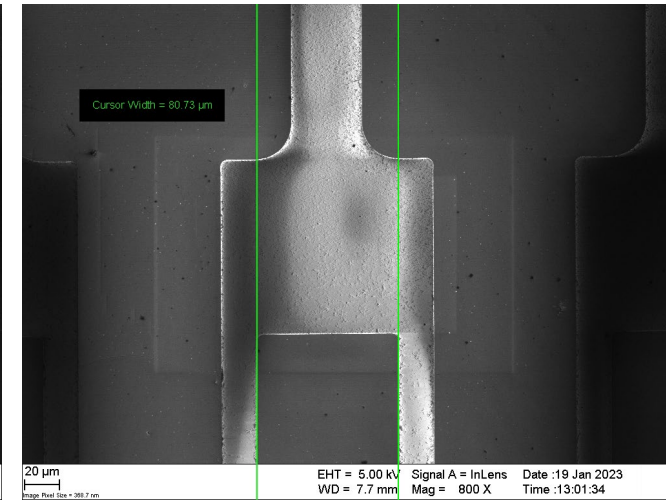
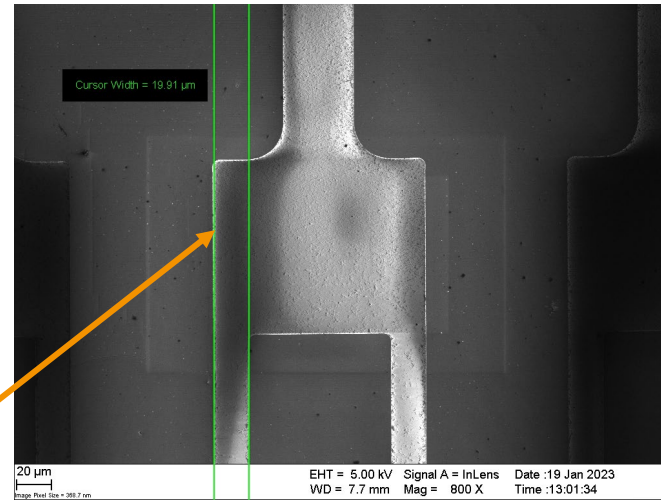


Sapphire 192-strip + FERS A5202
(CERN)



Sapphire wafers quality control

- Sapphire from several manufacturers tested
 - 4x150µm from UniversityWafer Inc. (USA)
 - 3x110µm from Wuppertal (Germany)
- Optical and AF microscopy are used to inspect the samples to characterize the metallization: **sizes, thickness, composition** and defects



* There is no difference between spectra 13 and 16. So, spectrum 16 has been shown only.

Detector characterization: CCE and resolution

- Detector **response** to incident radiation is measured by the **charge collection efficiency**

$$CCE \equiv \frac{Q_{collected}}{Q_{ionisation}}$$

defined as the ratio between the collected charge and the charge created by ionization by the incident radiation.

- In general, **change collection efficiency** depends on
 - 1 the external HV biasing E-field - **CCE(V)** ,
 - 2 the instantaneous ionization charge deposited (by the incident beam) - **CCE(Q)** ,
 - 3 the history of the detector (i.e., radiation damage causes permanent performance degradation) - **CCE(dose)** .
- **Reconstruction performance (resolution)** is measured by benchmarking detector profile with a reference system (i.e., a scintillator imaged by a camera).

Charge collection efficiency. Theory

- If we assume the following conditions to hold
 - The detector is planar (thickness d is negligible compared to other dimensions)
 - The transport properties and the electric field are uniform in whole volume of the sensor.
 - The free charge in stationary conditions is negligible and its generation, due to a photon (or a particle) absorption, is instantaneous.
 - Diffusion and detrapping phenomena are negligible and the number density of charge carriers decrease with time as $\sim e^{-t/\tau}$.

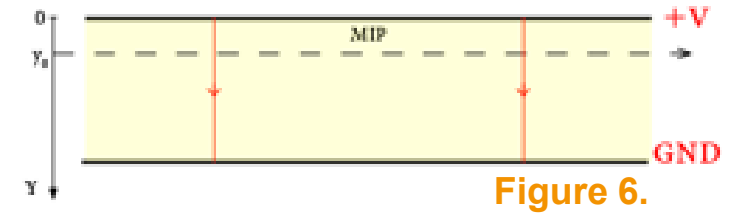


Figure 6.

alpha case

The CCE contribution from a localized initial charge deposited at y_0 is

$$\text{CCE}_e(y_0) = -\frac{f_d}{d} \cdot \int_{y_0}^0 dy e^{-\frac{y-y_0}{(\mu\tau)_e E_0}} = -V f_d \frac{(\mu\tau)_e}{d^2} \left(1 - e^{-\frac{y_0}{(\mu\tau)_e E_0}}\right) \quad (15)$$

$$\text{CCE}_h(y_0) = \frac{f_d}{d} \cdot \int_{y_0}^d dy e^{-\frac{y-y_0}{(\mu\tau)_h E_0}} = V f_d \frac{(\mu\tau)_h}{d^2} \left(1 - e^{-\frac{d-y_0}{(\mu\tau)_h E_0}}\right) \quad (16)$$

MIP case

If a uniform distribution of charge along a track (i.e., the MIP case) is considered, by integrating (15)+(16) over the thickness y_0 we get the CCE(V) we are looking for

$$\text{CCE}(V) = f_d k \left[1 + k \left(\exp\left(-\frac{1}{k}\right) - 1 \right) \right]$$

- $f_d \in [0,1]$ – the effective fraction of pairs propagating in sapphire;
- with $k \equiv \frac{\mu_e \tau_e}{d^2} V$

Charge collection efficiency. Theory

- If we assume the following conditions to hold
 - The detector is planar (thickness d is negligible compared to other dimensions)
 - The transport properties and the electric field are uniform in whole volume of the sensor.
 - The free charge in stationary conditions is negligible and its generation, due to a photon (or a particle) absorption, is instantaneous.
 - Diffusion and detrapping phenomena are negligible and the number density of charge carriers decrease with time as $\sim e^{-t/\tau}$.

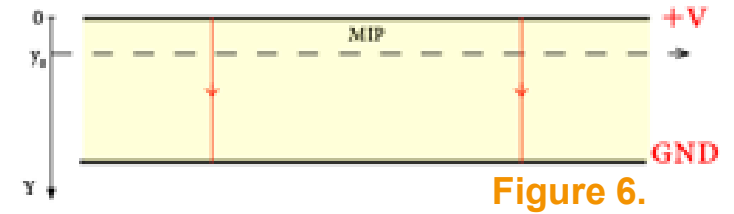


Figure 6.

alpha case

The CCE contribution from a localized initial charge deposit at y_0 is

MIP case

If a uniform distribution of charge along a track (i.e., the MIP thickness y_0) we get the CCE(V) we are looking for

$$\text{CCE}(V) = f_d k \left[1 + k \left(\exp\left(-\frac{1}{k}\right) - 1 \right) \right]$$

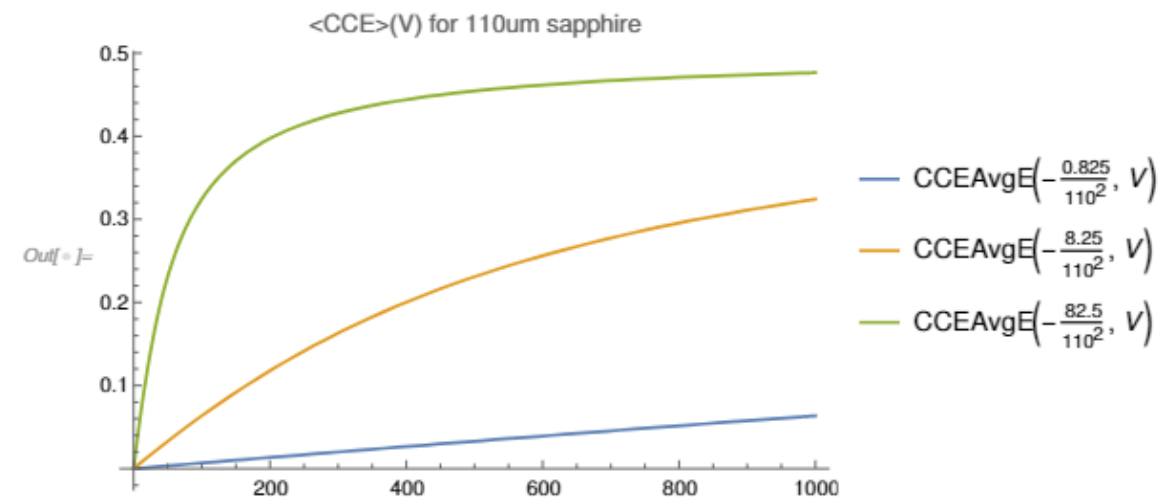


Figure 7. Plot of $\text{CCE}\left(\frac{\mu\tau}{d^2}, V\right)$ for a 110um planar detector with $-(\mu\tau)$ products of 0.825, 8.25, 82.5 $\mu\text{m}^2\text{V}^{-1}$ and $f_d = 1$.

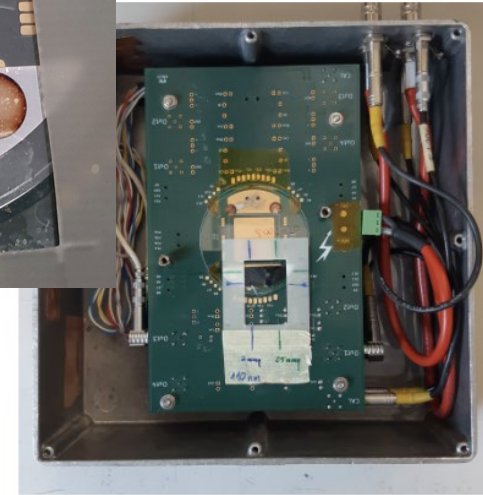
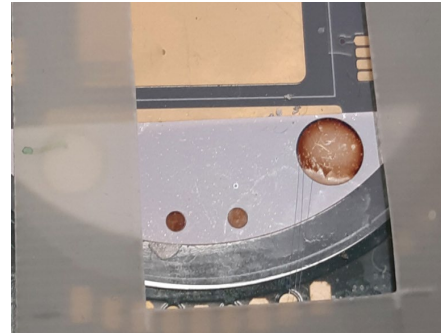
Test beams. Pad sensor test at Frascati INFN national laboratories

Goals

- Investigate sapphire CCE as a function of the **external biasing voltage**
- and **beam bunch charge**.

Setup

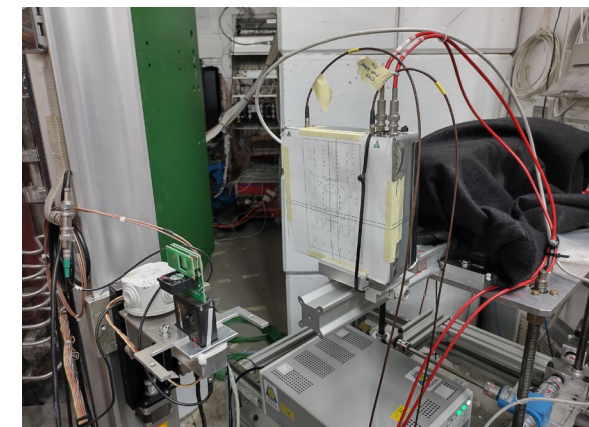
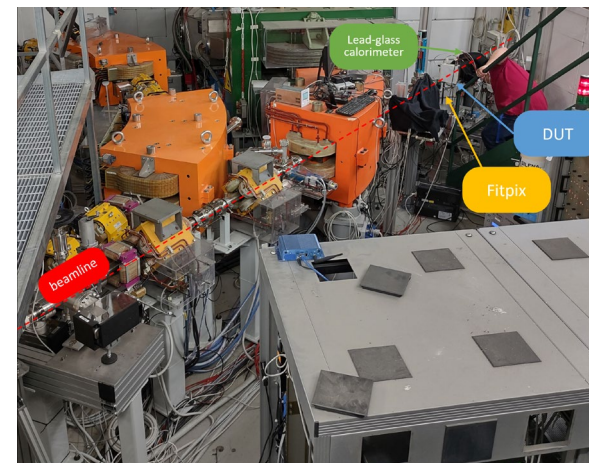
- 2-inch sapphire wafer with two metal-plated pads ($r_{SP} = 0.8\text{mm}$, $r_{LP} = 2.75\text{mm}$) on top surface. Two samples (thickness $110\mu\text{m}$, $150\mu\text{m}$) stacked one after the other in the DUT assembly.
- Strip LP/SP routed to independent 200mV/fC charge sensitive amplifiers and signal readout with a digital oscilloscope.
- In-air test with a 300MeV bunched e-beam ($1\text{-}10^5$ e/bunch, 10ns) monitored with a $400\mu\text{m}$ -thick silicon GP (upstream) and lead-glass calorimeter



(a) upstream (110)



(b) downstream (150)



Test beams. Pad sensor test at Frascati INFN national laboratories

Systematics

- Beam-DUT misalignments and air scatterings – evaluated by a Geant4 sim.
- Beam profile and charge not acquired – average values over 1k bunches used.

Results

- Typical efficiency of 14% (12%) for the 110 μm (150 μm) operating at 1kV.
- Typical charge carriers drift distance small w.r.t. the sensor thick. (*linear regime* of the CCE(V)).
- The $(\mu\tau)_e$ product is extracted from the fit:
 - for the 110 μm $(\mu\tau)_e \in 2.13 \pm 0.05 \mu\text{m}^2\text{V}^{-1}$
 - for the 150 μm $(\mu\tau)_e \in 2.93 \pm 0.05 \mu\text{m}^2\text{V}^{-1}$
- Linear dependence of CCE with beam bunch charge up to 40k e/bunch.
- Hints of residual field in the 110 μm -thick detector.

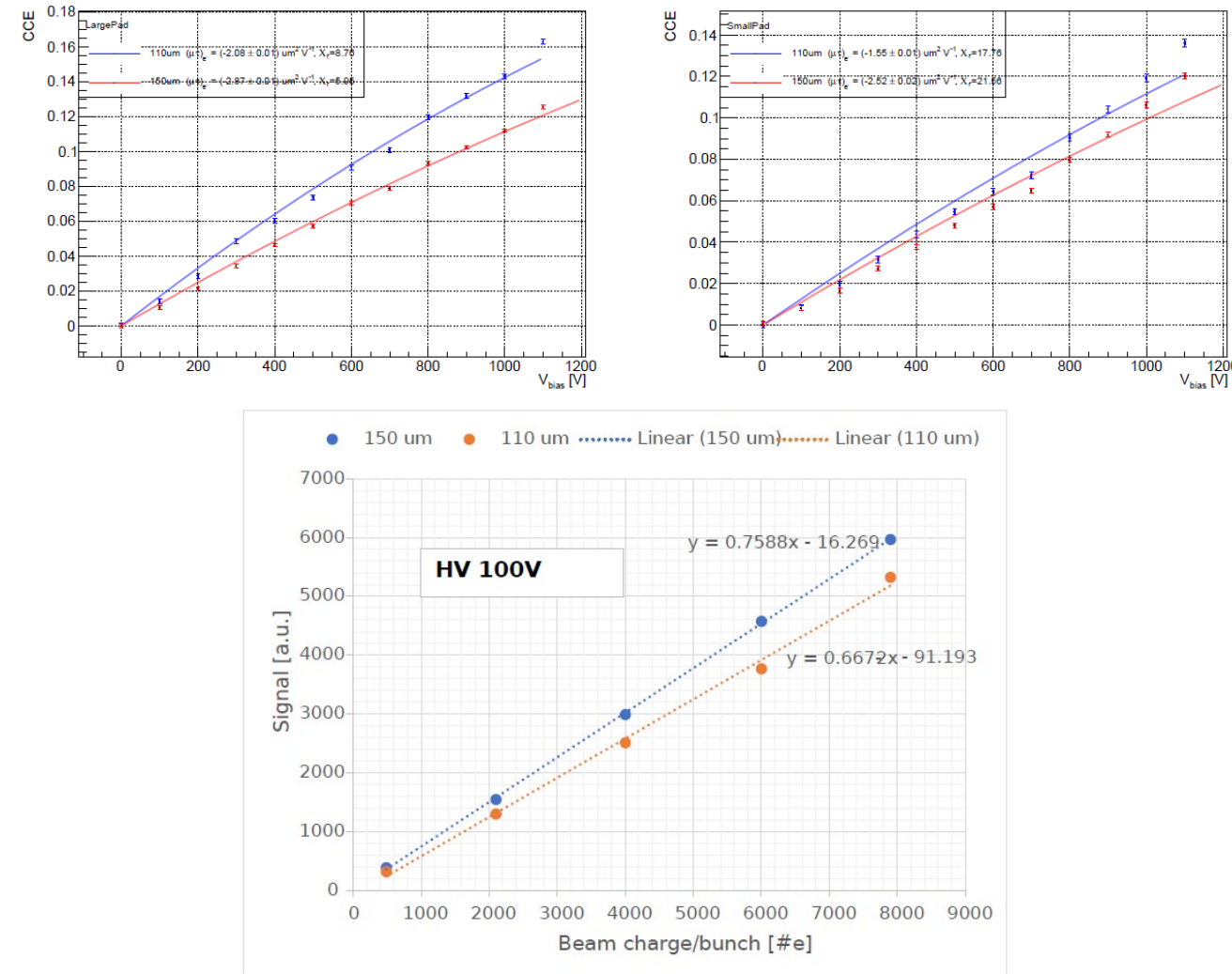

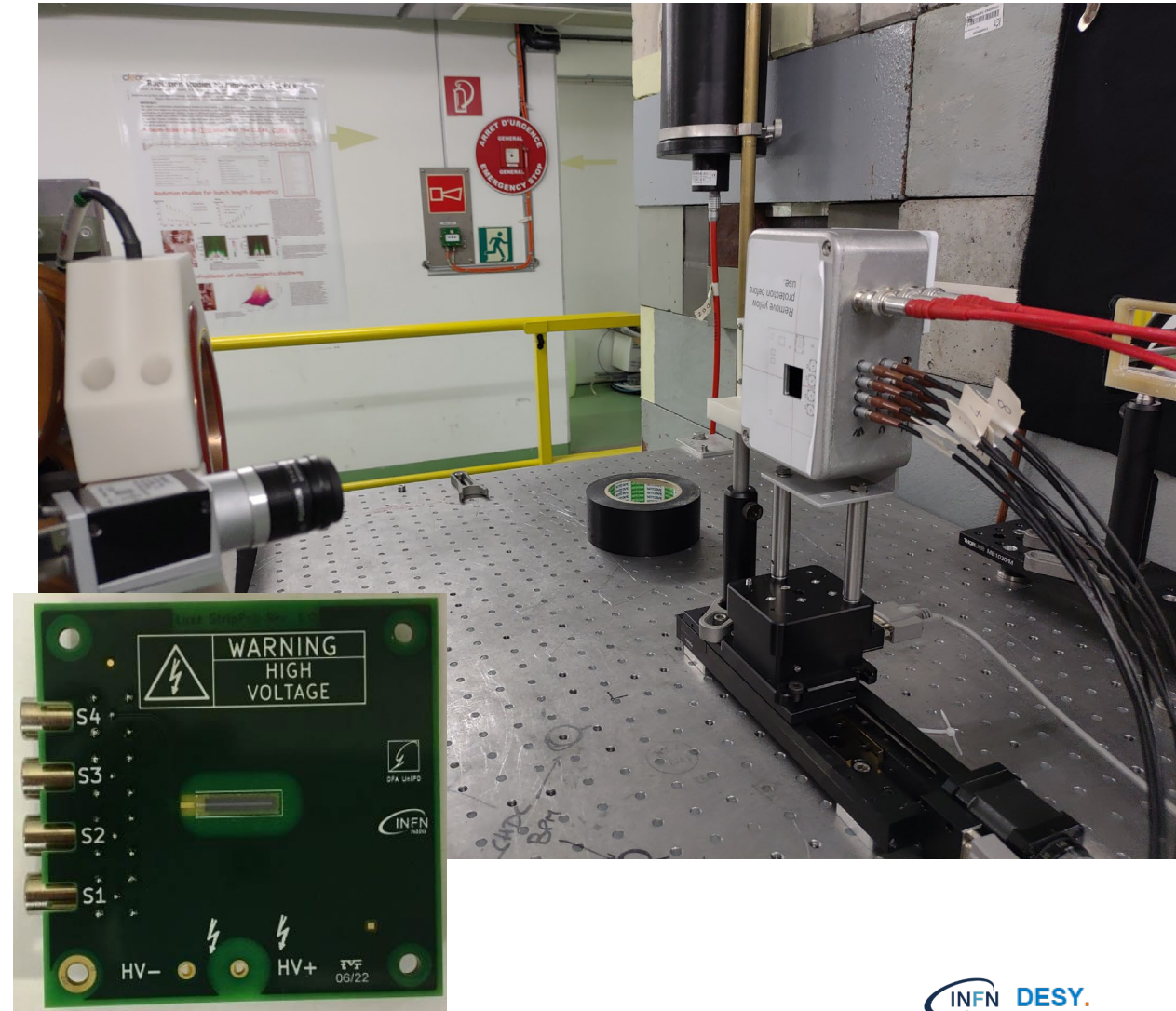


Figure 9.9: Behaviour of the collected charge from the large pad as a function of the beam multiplicity (inset <8ke), at a fixed bias voltage of $V_{bias} = 100\text{V}$. 

Test beams. Four-strip sensor. Scope and setup

- Tomsk 4-strip (80 μ m x 1cm) sensors have been tested at CLEAR (CERN) with an e-beam.
- CLEAR facility able to deliver charges 10pC - 270nC with a bunched electron beam (1-180 bunch/train) with gaussian 1x2 mm² profile, at a maximum train repetition rate of 10Hz.
- High beam charge allows **measurement of strip signals without any amplification**, directly at the strip **with an oscilloscope**.



Nb. channels	4	4	3 (1 not working)
Thickness	110um	150um	150um
Manufacturer	Wuppertal	University	M-type
Beam intercept	first	second	third



Test beams. Four-strip sensor.

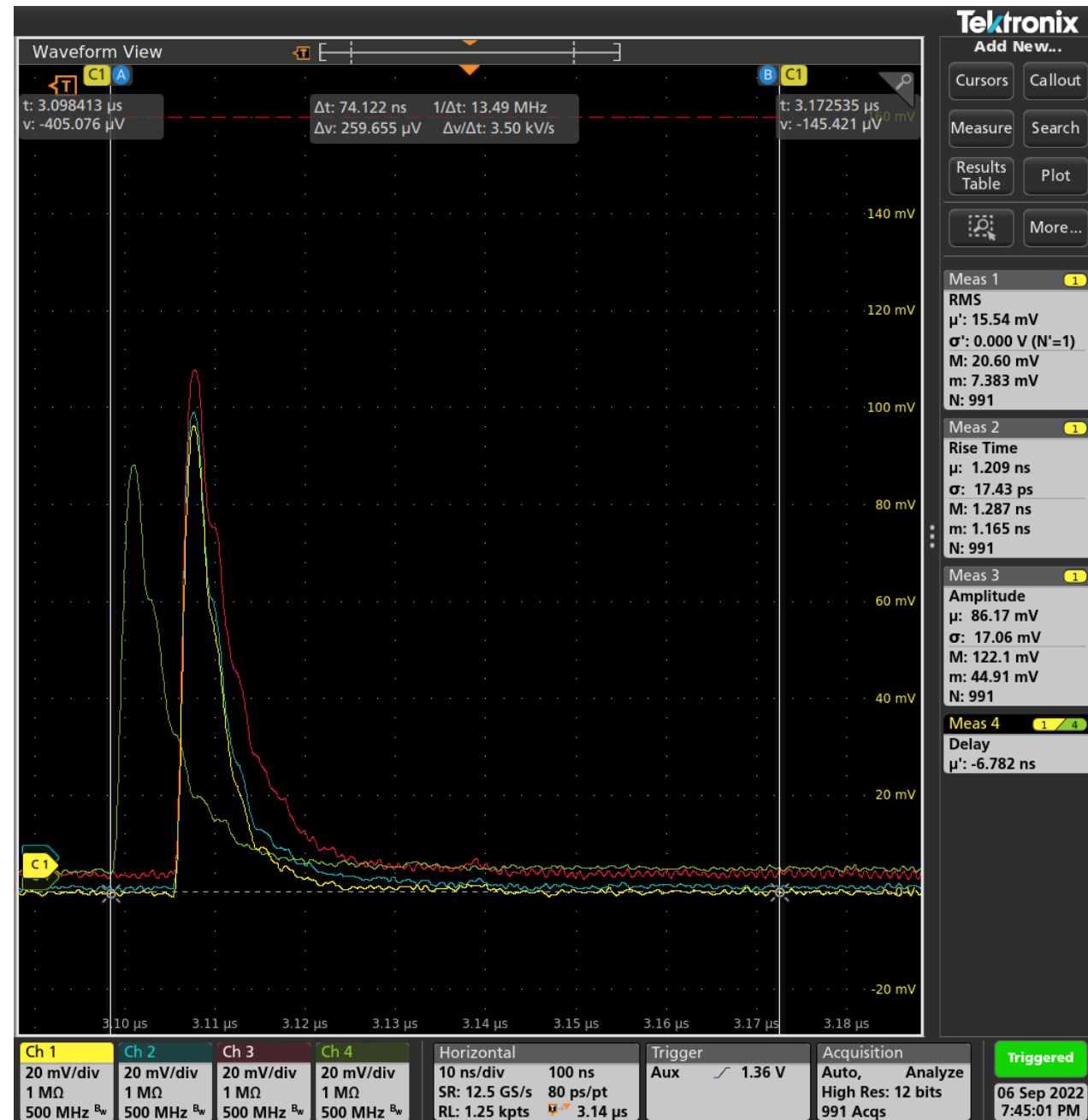
Main results

Investigated

1. Charge collection efficiency vs. HV-bias
2. Strip-response vs. beam position on the strip
3. Relative charge collected after high irradiation (15MGy)

Results

- Measurement of the bare signal produced in sapphire.
 - ▶ Very fast (ps) rise time.
- Sensor uniform response found.
 - ▶ Uniform charge collection along the strip.
- Relative CCE with irradiation behaviour.
 - ▶ Degradation observed, but systematics too large to extract dependence with dose.



Test beams. GBP 192-strip sensors. Scope and setup

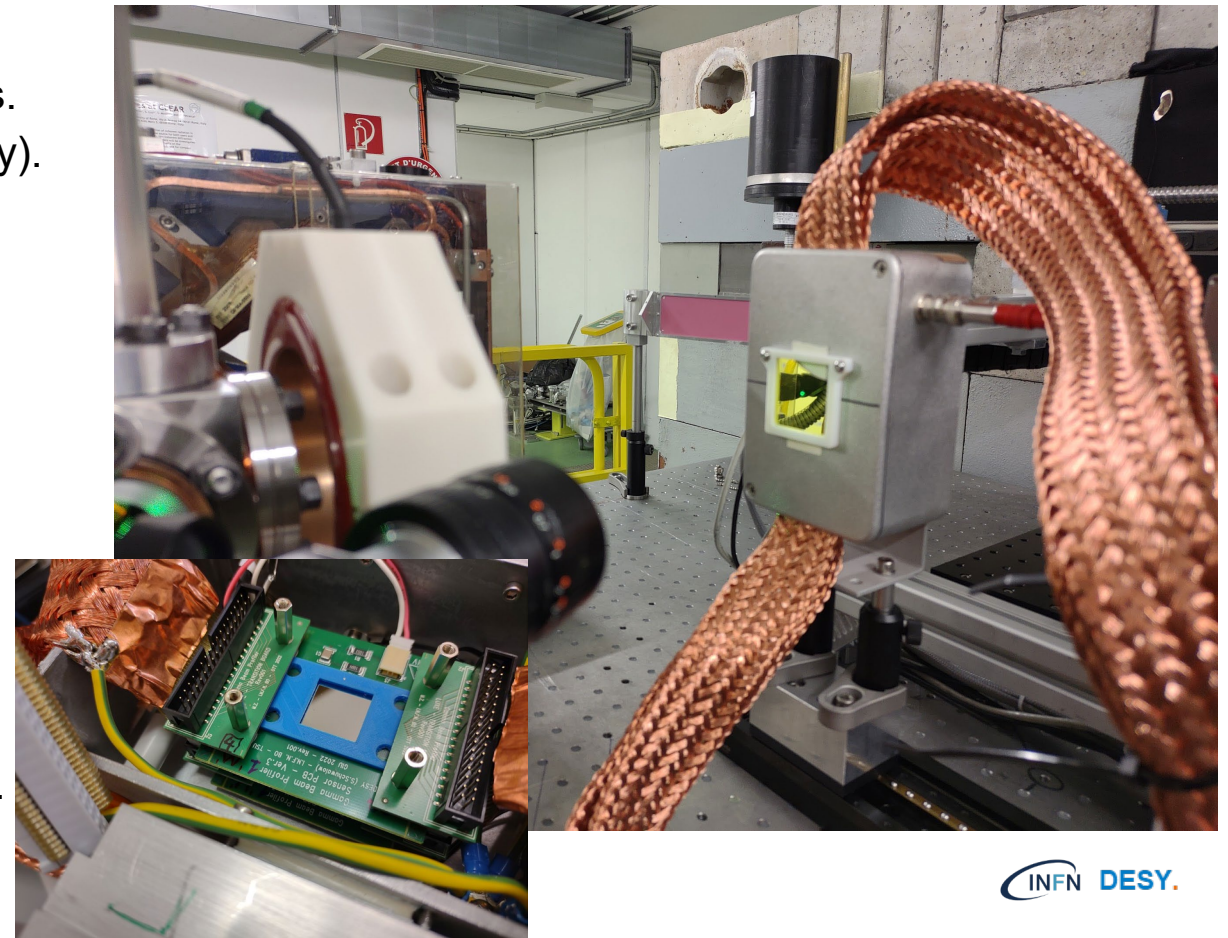
- Tomsk 192-strip (100 μ m pitch, 110 μ m-thick) sensors received Summer '22.
- Wire bonding made in Pisa, Italy.
- Tested at CLEAR (CERN) with an e-beam. March '23.

Goals

- First test of the electronics (PS, FERS).
- CCE(V), CCE(Q) and strip-response with beam pos.
- Relative CCE w.r.t. the dose delivered (up to 10MGy).
- BP reconstruction w.r.t. the scintillator screen.
- Signal/noise w.r.t. different grounding conf.s

Setup

- 2x192-strip 110 μ m (Monocrystal) and 150 μ m (UniversityWafersInc.) sensors tested.
- Ribbon shielded cables 3m used.
- Patch panel with **64ch** sensor **readout** by 2xFERS A5202 cards.
- Beam profile monitored with a scintillator and a camera, and beam charge acquired event by event.

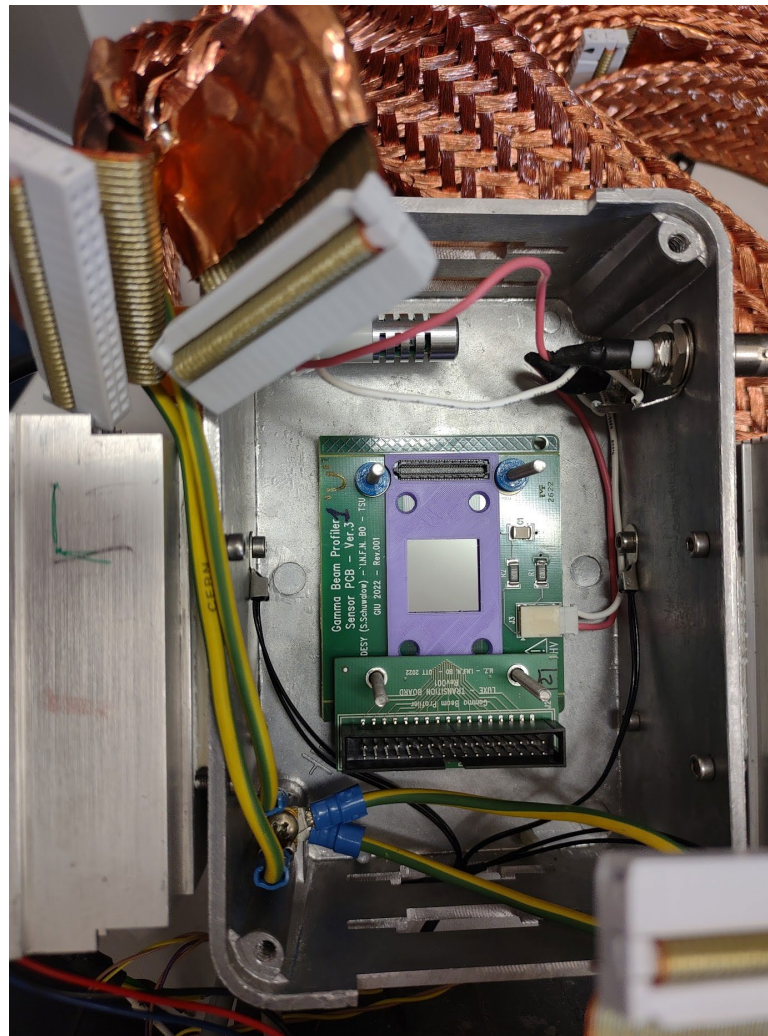


Test beams. GBP 192-strip sensors. Scope and setup

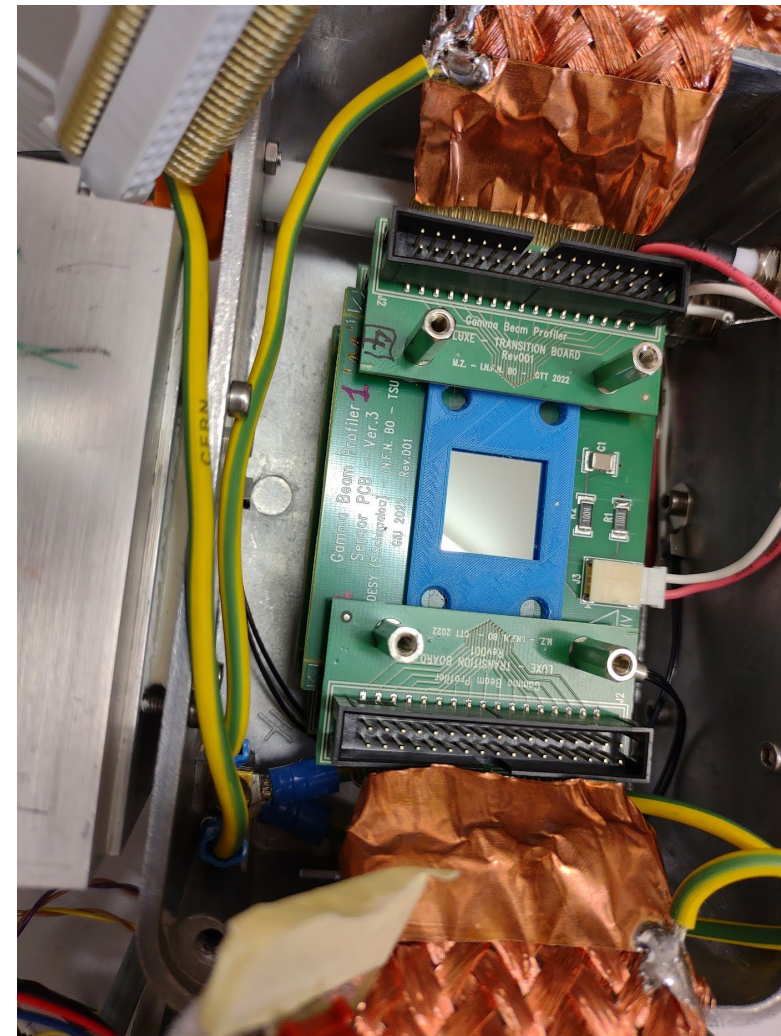
- Content of the box showing
 - the two sensors,
 - ground connections,
 - the transition boards (id),
 - humidity and thermocouple sensors (unused).

- **Upstream**
 - detector 1' **Monocrystal (110um)**
 - connected to **HV ch0 (2901709A)**
 - connected to **FERS det1 (pid24990)**

- **Downstream**
 - detector 1' **UniversityWafersInc. (150um)**
 - connected to **HV ch1 (2901710A)**
 - connected to **FERS det0 (pid22096)**



■ downstream

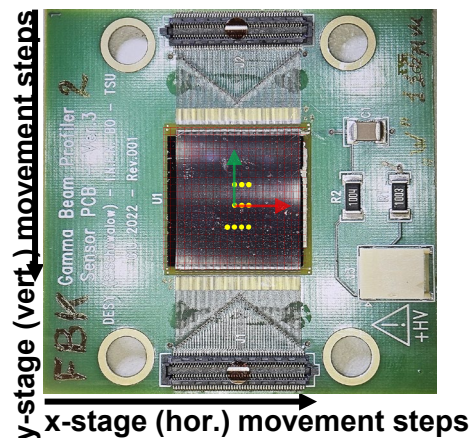
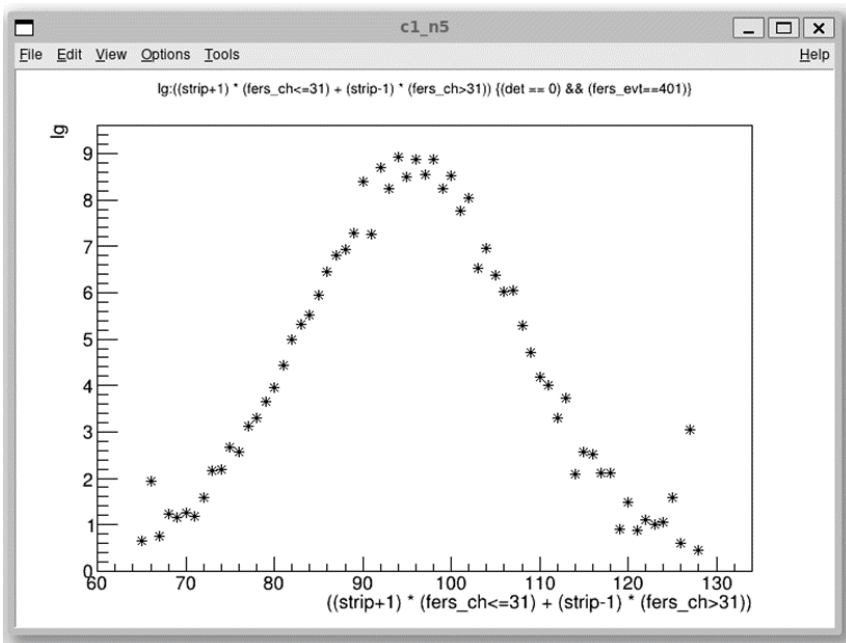


■ upstream

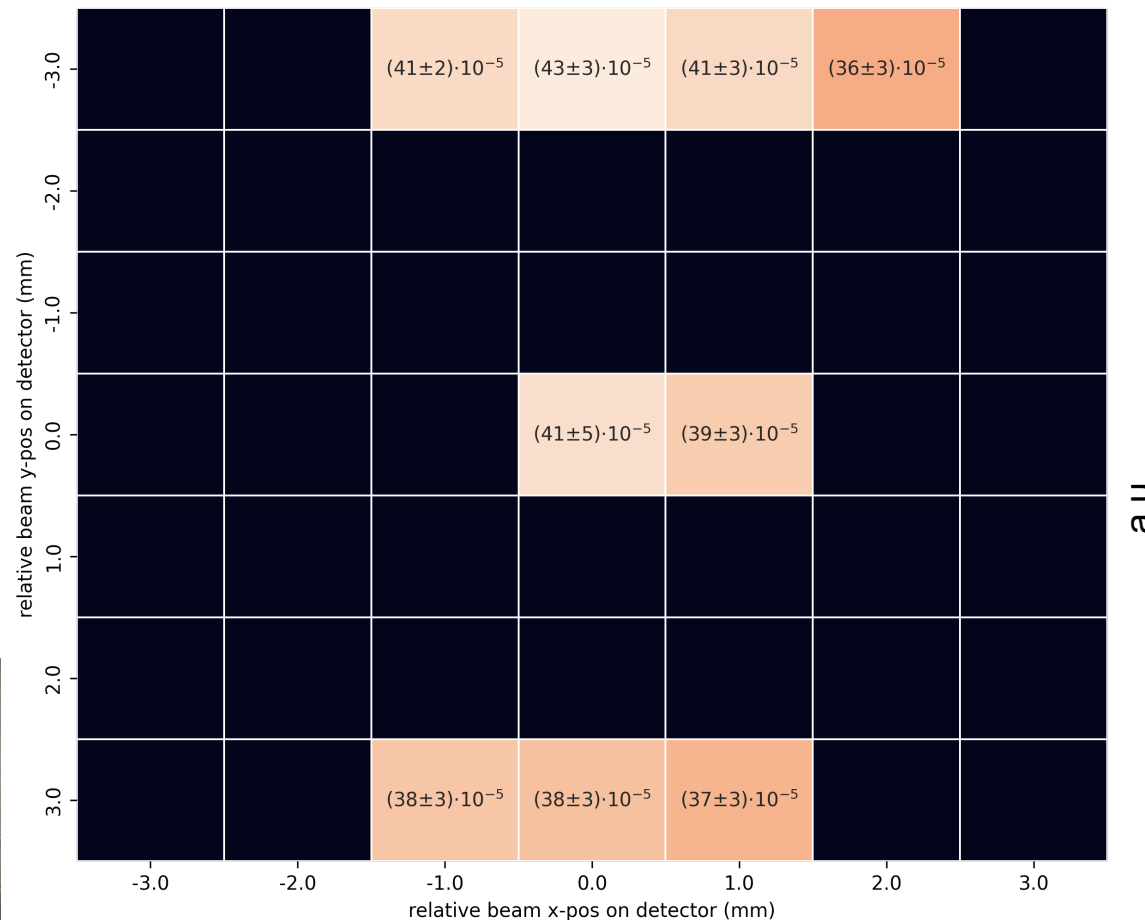
Test beams. GBP sensors. Results

Results (selection)

- First readout with FERS-A5202 of a sapphire microstrip sensor (64 strips).
- Uniform response in the sampled 12mm² area for both the wafers.



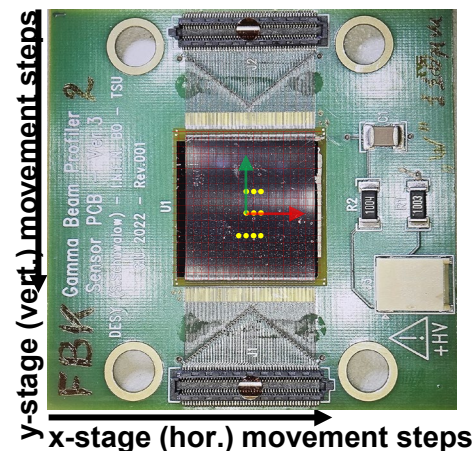
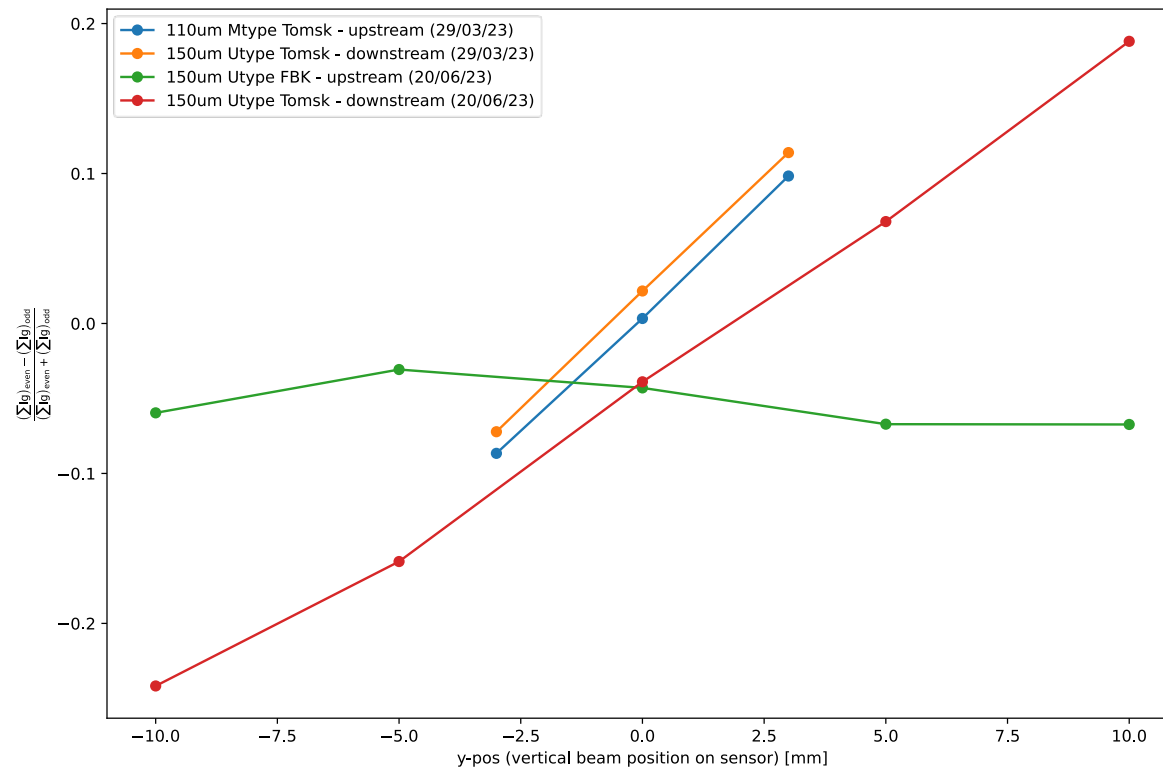
Ratio between (detector HV supply current) / (readout charge) (integral of readout gaussian profile) – upstream sensor



Test beams. GBP sensors. Results

Results (selection)

- First readout with FERS-A5202 of a sapphire microstrip sensor (64 strips).
- Uniform response in the sampled 12mm² area for both the wafers.
- Observed the effect of the strip high-resistivity (!) on the BP reconstruction in the asymmetry between even/odd profiles.

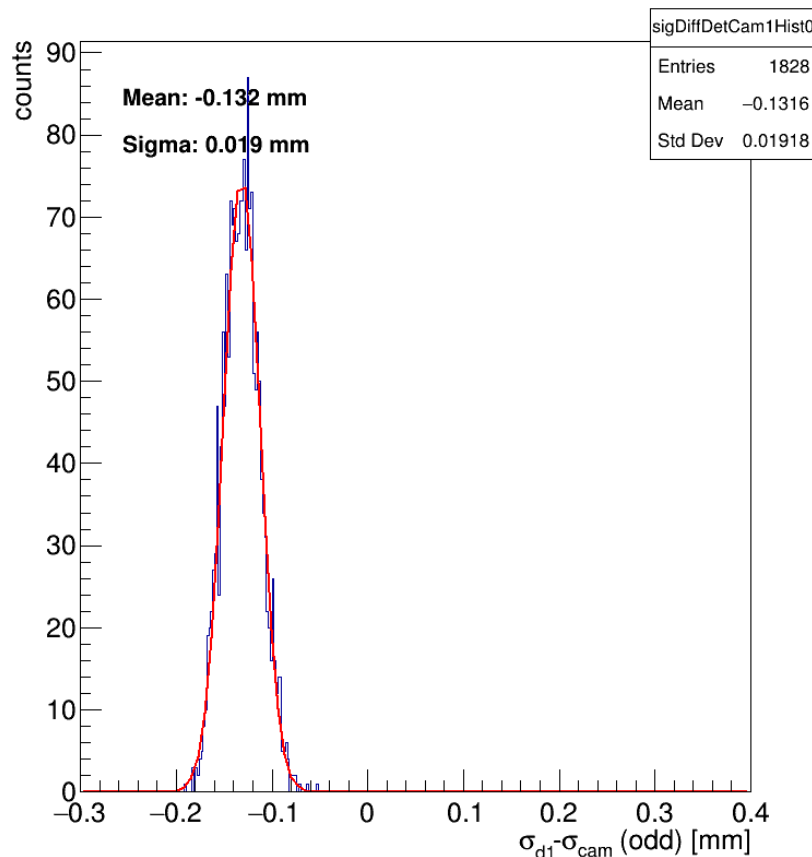
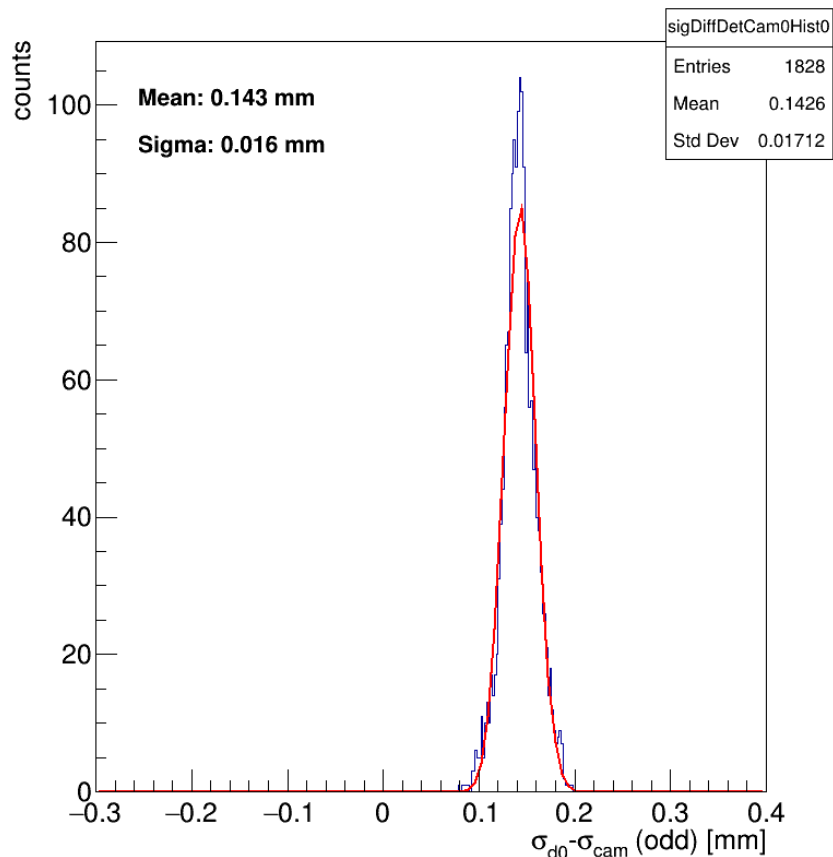




Test beams. GBP sensors. Results

Results (selection) – continued

- Preliminary assessment of statistical errors in measuring the electron beam profile in one direction, by comparison with the reference scintillator as imaged by the camera.



- Good results from the data taken with the sensors produced in Tomsk
 - 5-10 um statistical error
- Measurements to be repeated in the next test beam with the final FBK sensors.
- Measurements affected by significant systematic whose reasons are being investigated - i.e., cross-talk between the channels)

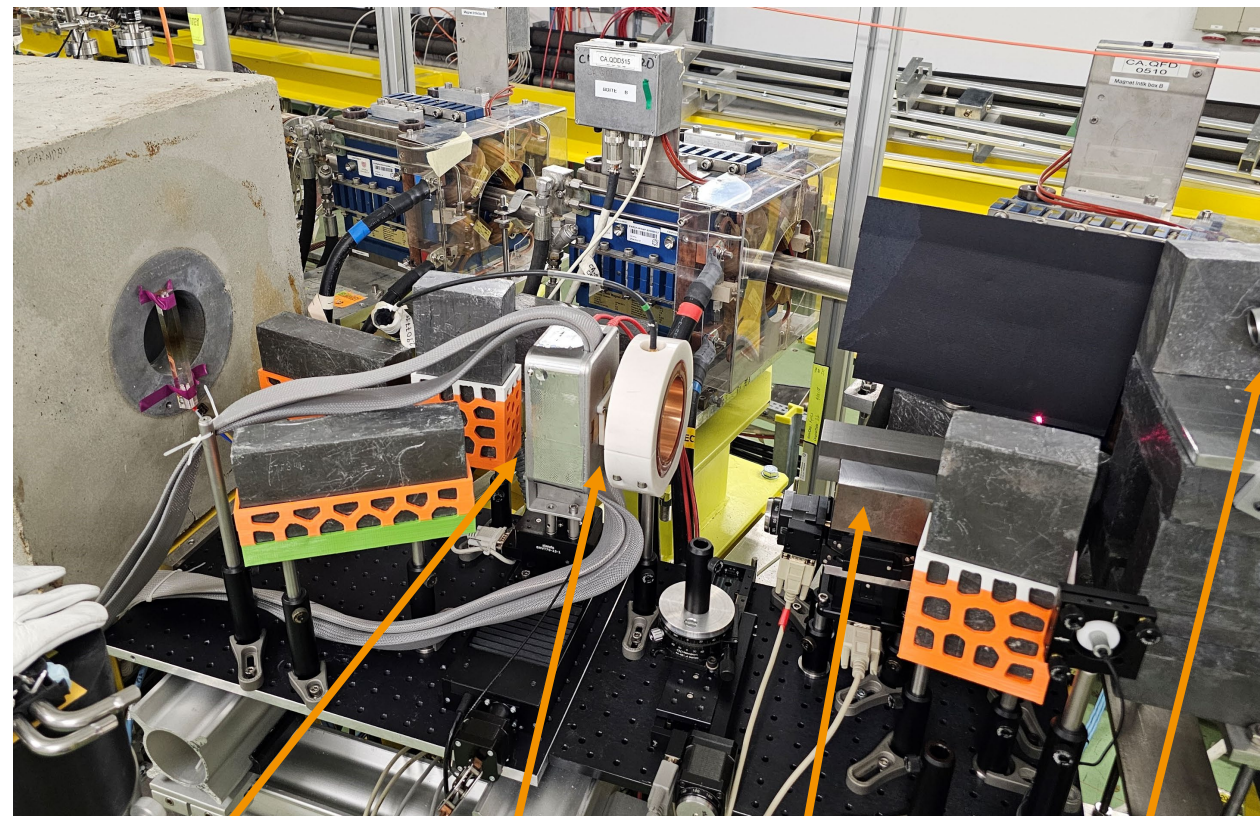
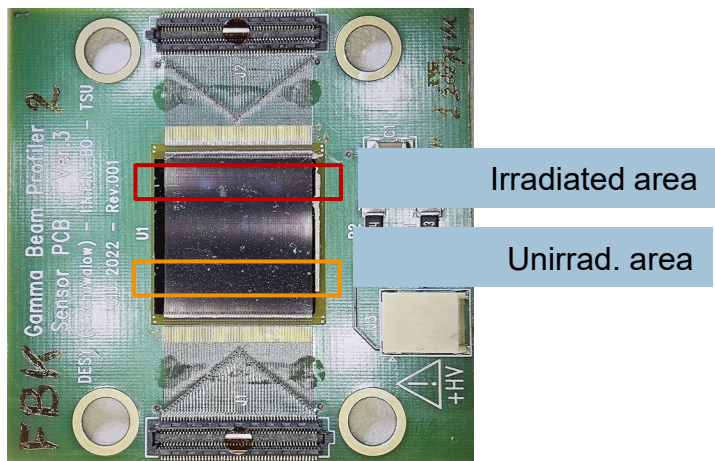
Test beams. GBP 192-strip sensors. Scope and setup

Goals

- Test of new FBK sensors (**strip resistivity**) under high irradiation (up to 10MGy).
- Measure detector response as a function of the radiation damage.

Setup (CLEAR, CERN)

- Stack of 2 parallel-oriented 192-strip FBK sensors.
- Tungsten collimator protecting half-sensor from irradiation.



Sapphire detectors

YAG screen

W collimator

camera

Test beams. GBP 192-strip sensors. Scope and setup

Setup (CLEAR, CERN)

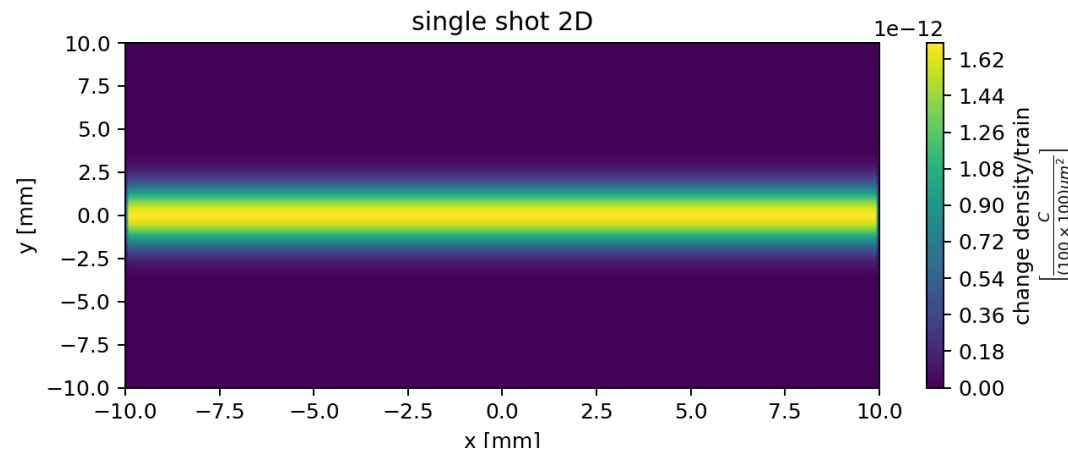
- Stack of 2 parallel-oriented 192-strip FBK sensors.
- Tungsten collimator protecting half-sensor from irradiation.
- Horizontal flat-top beam shape used for uniform detector irradiation in the upper part.



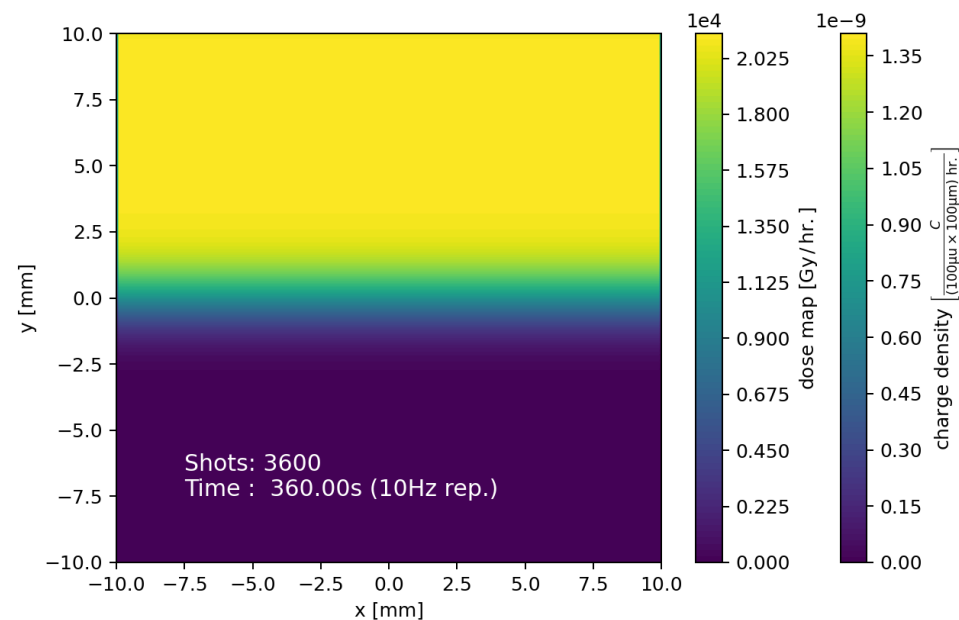
0 MGy



3.4 MGy



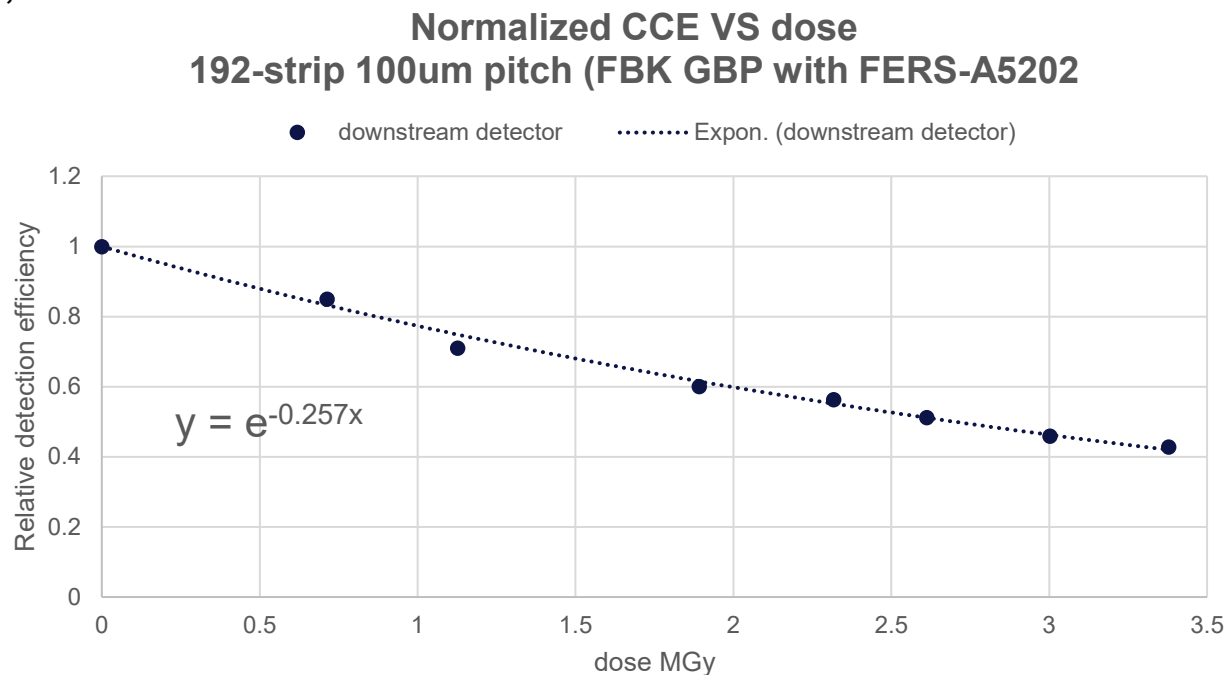
Accumulated charge/dose map in the sensor [bin size: 100um by 100um]



Test beams. GBP 192-strip sensors. Preliminary results (20/05/24)

- Analysis ongoing...
 - observed exp. degradation in relative detection efficiency due to radiation damage,
 - as expected from literature
<https://arxiv.org/abs/1504.04023>.

- Induced damage effect on resolution will be investigated in the next test beam at CLEAR (before summer shutdown).





Conclusions

- Managed to manufacture for the first time a microstrip sapphire detector.
- Solved early challenges in sapphire manufacturing. Developed a complete detector (GBP) for LUXE. Final prototype being tested and validated.
- Sapphire R&Ds reveal the sapphire sensors can be used as a suitable radiation-hard detector capable of measuring signals in wide range of beam released energy
 - from O(MeV) at HV=1kV...
 - ...to O(10 TeV) – or O(100 MIPS) at HV=50V
- MC simulations of sapphire sensor – Geant4 and Allpix2 – developed and validated on the literature.

Thank you!